

# eScholarship@UMassChan

## T Cell Lymphopenia in Severe Congenital Neutropenia Type 5 Mouse Model

Item Type	Master's Thesis
Authors	Norris, Kristyn
DOI	<a href="https://doi.org/10.13028/y84h-zm89">10.13028/y84h-zm89</a>
Publisher	UMass Chan Medical School
Rights	Copyright © 2025 Kristyn Norris
Download date	2026-04-15 13:01:16
Item License	<a href="https://creativecommons.org/licenses/by/4.0/">https://creativecommons.org/licenses/by/4.0/</a>
Link to Item	<a href="https://hdl.handle.net/20.500.14038/54408">https://hdl.handle.net/20.500.14038/54408</a>

T CELL LYMPHOPENIA IN SEVERE CONGENITAL NEUTROPENIA TYPE 5 MOUSE  
MODEL

A Master's Thesis Presented

By

Kristyn Marie Norris

Submitted to the Faculty of the  
Morningside Graduate School of Biomedical Sciences at UMass Chan Medical School

In partial fulfillment of the requirements for the degree of

MASTER'S OF SCIENCE

(April 16, 2025)

(Biochemistry and Molecular Biotechnology)

T CELL LYMPHOPENIA IN SEVERE CONGENITAL NEUTROPENIA TYPE 5 MOUSE  
MODEL

A Master's Thesis Presentation

By

Kristyn Marie Norris

The signatures of the Master's Thesis Committee signify completion and approval as to style and content of the Thesis.

Mary Munson Ph.D., PI

Kate Fitzgerald Ph.D., Chair of Committee

Ann Rothstein Ph.D., Member of Committee

Daryl Bosco Ph.D., Member of Committee

The signature of the Dean of the Graduate School of Biomedical Sciences signifies that the student has met all master's degree graduation requirements of the school.

Mary Ellen Lane, Ph.D.,

Dean of the Graduate School of Biomedical Sciences

Biochemistry and Molecular Biotechnology

April 16, 2025

## Dedication

I want to dedicate this work to all those I have lost in the process, my mother, Francine Sylvie Lareau Norris, and my sister Heather Lise Norris. I wouldn't have made it so far without your unwavering love and support. I would also like to dedicate this to the rest of my family who have been so supportive along this journey. Additionally, all the friends whom I have made along the way and who inspire me to be my best self, Ginger, Tyler, Mike, Alyssa, Miri, Halsey, Monika, and more. Also, to my best friends who haven't seen too much of me over the years but still stay strong in our friendships, Rachel and Hanna. Finally, my lab mates and PI, whom I couldn't have done this without, Dr. Mary Munson, Dante, Leo, and more.

## **Acknowledgements**

Collaborators: Zhiqing (Julie) Zhu, Josias Brito Frazão, Peter Newburger, Kate Gordon

Former lab members: Dante Laporte, Jenifer Forcina, Alex, Alex, Madeline, Jackie, Mike Feyder, Mary Munson, Kimmie, Brenda

Current members of the lab: Helen, Rinalda, Natasha, Havi, Melonnie

Ann Rothstein's lab: Kevin Gao

EM core - Award # is S10 OD025113-01

SCOPE Imaging core

Transgenic Animal Modeling Core

FACS core

## **Abstract**

VPS45 is a regulator of membrane trafficking. Severe Congenital Neutropenia Type 5 (SCN5) is associated with mutations in VPS45. VPS45 is ubiquitously expressed, while SCN5 is characterized by a reduction in neutrophils. The focus of this work is to discover the link between VPS45 and SCN5. In collaboration with the Newburger lab, a mouse model of the SCN5 mutation was created. Initial discoveries of the mouse model parallel the SCN5 phenotype, failure to thrive, with lower weights and a smaller appearance. It was discovered that T cell lymphopenia was the primary effect of these VPS45 KI mutations. The VPS45 mutant T cells have a more activated phenotype. The development of the VPS45 mutant T cells were abnormal, lacking some of the initial stages of development in the thymus. This work, although preliminary, illuminates the importance of VPS45 and proper membrane trafficking in immune cells.

**Table of Contents**

<b>Chapter</b>	<b>Title</b>	<b>Page</b>
CHAPTER I	Introduction	1
CHAPTER II	Creation of the mouse model and initial discoveries	13
CHAPTER III	The SCN5 phenotype is present in the VPS45 KI mouse model	17
CHAPTER IV	VPS45 KI mice have T cell lymphopenia	24
CHAPTER V	VPS45 KI mice have abnormal thymi	31
CHAPTER VI	Preliminary data suggest T cell lymphopenia is intrinsic	35
CHAPTER VII	Discussion	37
	Methods and materials	40
	Bibliography	44

## List of Figures

<b>Figure</b>	<b>Title</b>	<b>Page</b>
Figure 1	Simplified Membrane Trafficking Model	2
Figure 2	SNARE Complex Formation	4
Figure 3	VPS45 Interacts with Syntaxin 16	7
Figure 4	Model of SCN5-associated VPS45 Mutations	9
Figure 5	RNA and Protein Expression of VPS45 in Humans	11
Figure 6	Body Weights of VPS45 KI Mice are Significantly Less	14
Figure 7	CBC of SCN5 Mouse Model at Early Ages	15
Figure 8	Non-Mendelian Ratios from a Heterozygous Cross	16
Figure 9	Gating Strategy for Flow Cytometry	18
Figure 10	VPS45 KI Mice Displayed SCN5 Patient Phenotype	20
Figure 11	VPS45 KI Mouse Neutropenia was Observed in Every Organ Probed	21
Figure 12	VPS45 KI Mice had Fewer Myeloid Cells	22
Figure 13	VPS45 KI Mice Neutrophil EM Reveal Similar Numbers of Granules and Morphology Compared to WT Neutrophils	23
Figure 14	Gating Strategy for Flow Cytometry of T cell Subpopulations.	25
Figure 15	VPS45 KI Mice had Severe T cell Lymphopenia	26
Figure 16	CD8 T Cell TEM Reveal Wildtype Appearance of VPS45 KI Mice CD8 T Cells	27
Figure 17	Additional Lymphocyte Populations Probed Show More Lymphocytes in VPS45 KI Mice	28
Figure 18	VPS45 KI Mice had Skewed T cell Subsets	29
Figure 19	VPS45 KI Mice have an Activated Phenotype	30
Figure 20	Thymus Flow Panels	32
Figure 21	VPS45 KI Mice have an Abnormal Thymocyte CD4 and CD8 Landscape	33
Figure 22	VPS45 KI Mice have a Skewed Double Negative Profile	34
Figure 23	VPS45 KI Lymphopenia and Decreased White Blood Cells are Cell Intrinsic	36

### List of symbols, abbreviations, and nomenclature

<b>Symbol/Abbreviation/Nomenclature</b>	<b>Meaning</b>
ER	Endoplasmic reticulum
TGN	Trans Golgi Network
SNARE	Soluble NSF attachment protein receptors
t-SNARE	Target SNARE protein
v-SNARE	Vesicle SNARE protein
Q-SNARE	SNARE protein that contributes a glutamine to the zero layer
R-SNARE	SNARE protein that contributes an arginine to the zero layer
SNARE complex	4-helical bundle with 4 SNARE motifs
SM protein	Sec1/Munc18 protein
stx	Syntaxin
SCN5	Severe Congenital Neutropenia type 5
rbsn5	Rabenosyn 5
G-CSF	Granulocyte colony-stimulating factor
TEM	Transmission electron microscopy
CBCs	Complete blood counts
WT	Wildtype
KI	Knock In
HET	heterozygous
DN	double negative
FHL-4	familial hemophagocytic lymphohistiocytosis type 4

## CHAPTER I. Introduction

### Membrane Trafficking

Membrane trafficking is the process by which cargo, lipids, and membrane proteins move throughout the cell. Membrane trafficking is necessary for the survival and function of the cell. The cell has two major membrane trafficking pathways, endocytosis and exocytosis. Exocytosis is the process by which cargo, lipids, and membrane proteins travel through the ER and Golgi to their final destination on the outer membrane of the cell or outside the cell. Endocytosis is the process of internalization of cargo, lipids, and membrane proteins. These internalized molecules can have various destinations in the cell depending on what the cargo is. Endocytosis and exocytosis can be further split into specific rudimentary compartments based on which membrane process is occurring (**Figure 1**). These pathways are defined by the destination of the cargo. There is the recycling pathway that consists of the endocytosis of cargo, lipids, or membrane proteins through the endosomal system back out to the outer membrane. The lysosomal pathway is where cargo is moved through the cell to the lysosome for degradation. Endosomal pathway where cargo travels through the endosomal system to the outside of the cell, to be recycled or degraded. The Trans Golgi Network, TGN, is the process of traveling through the Golgi system, often leading to exocytosis. While this seems like a very straightforward concept, as illustrated by Figure 1, the cell is densely packed, requiring many factors to make sure cargo gets where it is supposed to go at the proper time<sup>1,2</sup>.

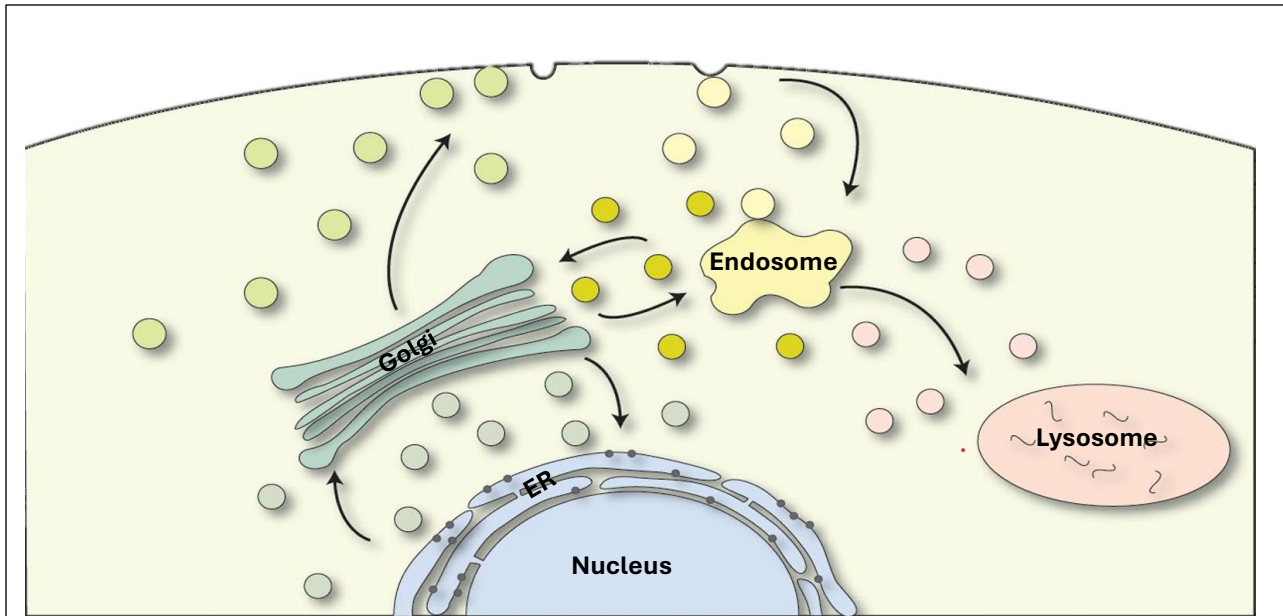
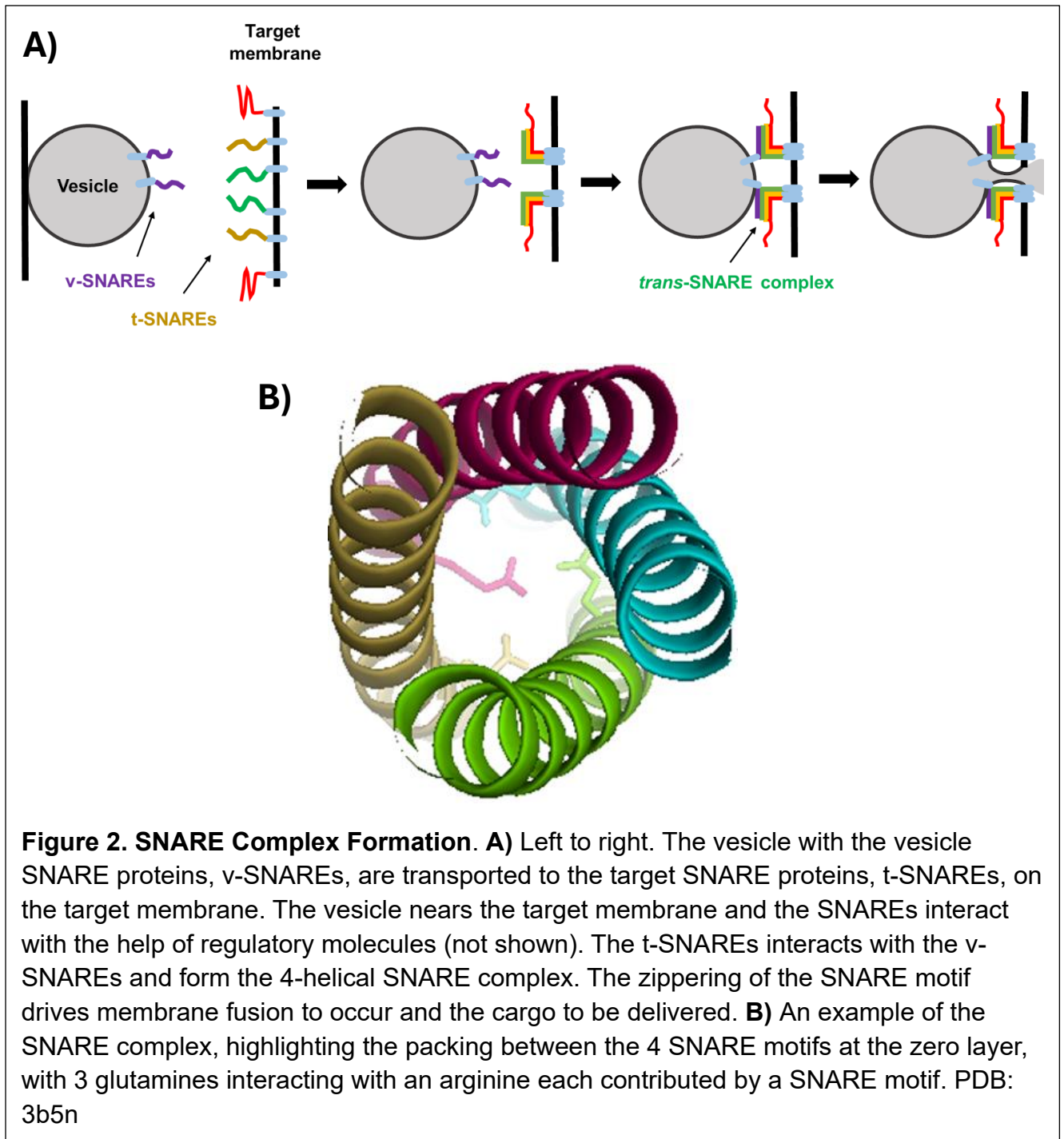


**Figure 1. Simplified Membrane Trafficking Model.** Endocytic and Exocytic membrane trafficking pathways are labeled with arrows. The recycling pathway (light yellow), endocytic pathway (dark yellow), lysosomal pathway (pink), trans Golgi network (green forward arrow), retrograde trafficking (green reverse arrow) and exocytosis (green-yellow) are all labeled in different colors. This is a very simplified version of the cell, in a real cell the cytoplasm would be filled with various macromolecules and other organelles. Membrane trafficking requires many different molecules working together to be successful.

## SNARE Proteins in Membrane Trafficking

At the core of membrane trafficking is membrane fusion mediated by soluble NSF attachment protein receptors (SNARE) proteins (**Figure 2**). Without SNARE proteins fusion would not occur. SNARE proteins are a group of integral and peripheral membrane proteins that possess a SNARE motif. The SNARE motif is the part of the SNARE protein that interacts with other SNARE proteins forming the SNARE complex, a 4-helical bundle. Without the SNARE motif, fusion would not be able to overcome the barriers of membrane fusion, including the energy requirement for such a process. When a SNARE motif interacts with other SNARE motifs, a coiled-coil or the 4-helical bundle is formed (**Figure 2b**)<sup>3</sup>. Complex formation is mediated through the zippering of the SNARE motifs, with the contribution of SNARE motifs from 3-4 SNARE proteins (**Figure 2 a and b**)<sup>4</sup>. The requirement of these additional SNARE motifs positions fusion to occur only when the membranes are in proximity of each other. The SNARE complex consists of 16 layers of hydrophobic residues with the exception of the core zero layer. At the zero layer, each SNARE motif contributes an arginine or 1 of 3 glutamine, creating a QabcR layer, adding another level of regulation<sup>4,5</sup>. While traditional nomenclature identifies these SNARE proteins as either target SNARE proteins, t-SNAREs and vesicle SNARE proteins, v-SNAREs, the literature has changes to calling them by which amino acid contributes to the zero layer, Q-SNARE or R-SNARE. Many syntaxin proteins, a subset of SNARE proteins, also contain regulatory elements, including a Habc domain and a N-peptide. These additional features allow for further regulation of SNARE complex formation. It has been proven that the Habc domain has an inhibitory role, folding into a 4-helical bundle with the SNARE motif and excluding it from interacting with other SNARE motifs. The role of the N-peptide is still elusive; however, it is proposed to be important in the interactions of the SNARE proteins with their regulators<sup>6-22</sup>. Although SNARE proteins are sufficient *in vitro* to form SNARE complexes, they can be promiscuous forming nonviable SNARE complexes, other factors are necessary for formation, fusion, and specificity *in vivo*,<sup>4, 23, 24</sup>.

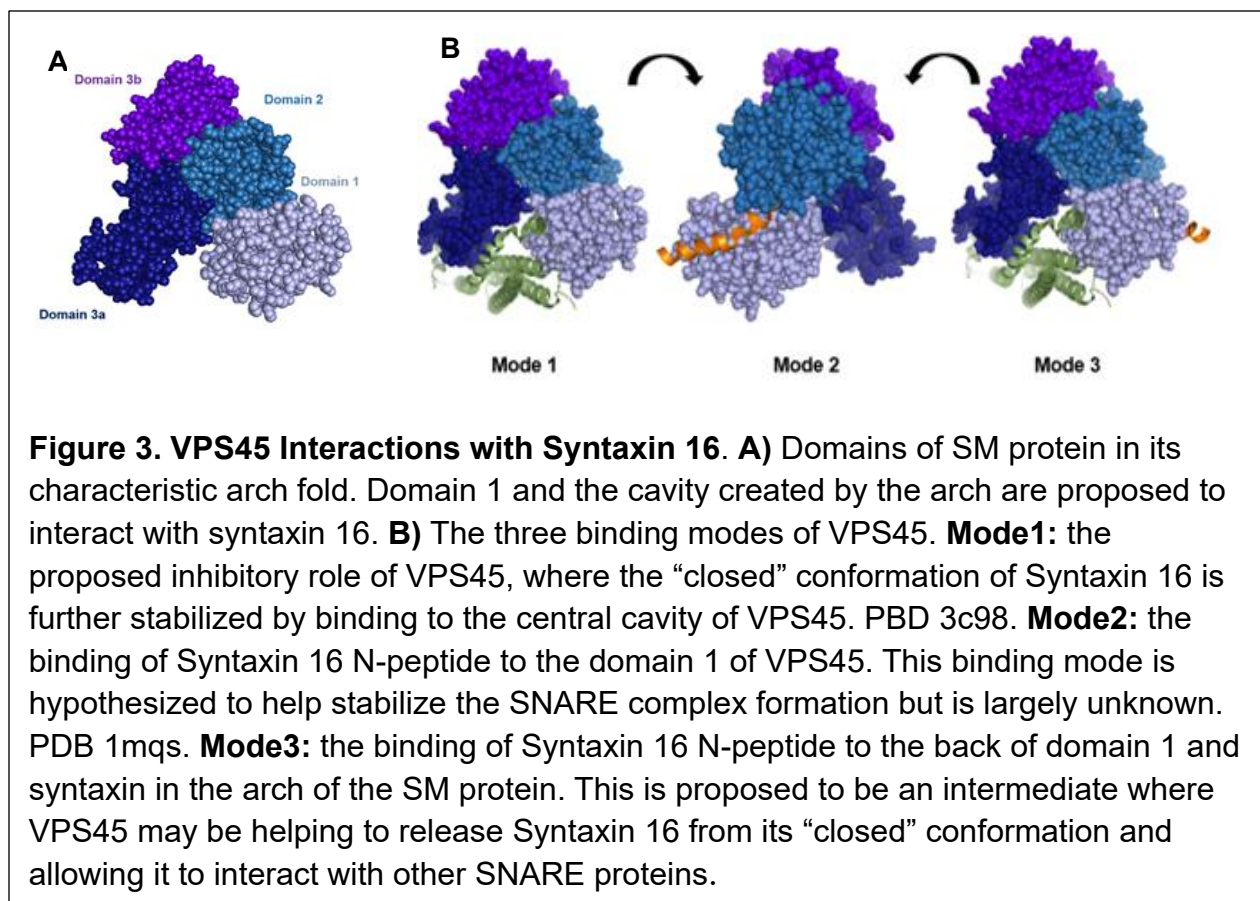


## SNARE Complex Regulation and Sec1/Munc18 Proteins

SNARE complex formation is regulated by a wide variety of proteins, including Sec1/Munc18 proteins. Sec1/Munc18 (SM) proteins are regulatory factors that bind to syntaxins or SNARE complexes and help dictate SNARE complex formation<sup>8-10,17-19, 25-29</sup>. SM proteins are all 600-700 residue cytosolic proteins that consist of 3 domains and characteristic arch shape (**Figure 3**)<sup>8-10,17-19, 25-29</sup>. SM proteins are classified into subfamilies based on their identification in yeast; Sec1/Munc18, Sly1, Vps33, and Vps45, each acting on a specific stage of membrane trafficking; exocytosis, ER/Golgi trafficking, lysosomal trafficking, and endosomal/recycling, respectfully<sup>28</sup>. SM protein's mode of action varies widely. Sec1 hasn't been shown to bind its cognate syntaxin but instead binds the fully formed SNARE complex<sup>23</sup>. VPS33 binds its syntaxin but works within a larger complex<sup>30</sup>. Sly1 binds its cognate syntaxin<sup>31</sup>. While VPS45's mode of binding is proposed to be similar to Sly1<sup>32</sup>. SM proteins are proven to use the cavity of their characteristic arch shape and a deep groove on the opposite face to bind either their cognate syntaxin or SNARE complex (**Figure 3**)<sup>9,28</sup>. SM proteins were initially discovered through the isolation of Munc18 bound to its cognate syntaxin, syntaxin 1<sup>33</sup>. Co-crystallization of Munc18 and syntaxin 1 revealed an inhibitory role for SM proteins (**Figure 3 mode 1**). The syntaxin was in its excluded conformation with its Habc domain forming a 4 helical bundle with its SNARE motif. This "closed" syntaxin conformation was understood to be further stabilized by being held in the central cavity of the Munc18<sup>9</sup>. This led to the hypothesis that SM proteins are inhibitory to SNARE complex formation. On the contrary, when deletion and knock down studies were done, the data showed that SM proteins are necessary for proper membrane fusion<sup>13, 25, 27, 34</sup>. These SM deletions were able to be rescued by "open" mutants of the cognate syntaxins. This, and other evidence, led to the hypothesis that SM proteins are necessary for the transition of syntaxins from the "closed" to the "open" conformation<sup>9,13,18, 35, 36</sup>. Research from our lab and others have further indicated that VPS45 may be used to "open" the closed syntaxin, syntaxin 16 (stx16), suggesting that VPS45 serves as a template for SNARE complex formation<sup>32</sup>. VPS45 research has also shown various binding modes between VPS45 and syntaxin 16 (**Figure 3**). VPS45 interacts with the "closed" conformation of stx16 further stabilizing this "closed" conformation and inhibiting SNARE complex formation (**mode 1**)<sup>9, 13, 14, 19, 27, 25, 37, 38</sup>. VPS45 binds to the N-peptide of stx16 to help stabilize SNARE complex formation (**mode 2**)<sup>9, 39</sup>. The N-peptide (1-33) of syntaxin 16 is sufficient for VPS45 binding and inserts into the opposing deep groove in the VPS45 structure<sup>9, 39</sup>. This additional role for N-peptide binding is likely to localize VPS45 and participate in SM-SNARE complex binding<sup>17, 38</sup>. And it is also possible that the two modes could happen at once, where the N-peptide of stx16 binds to domain 1 of VPS45 and the Habc and SNARE motif of stx16 in the central cavity of the VPS45 (**mode 3**) (**Figure 4**). VPS45 can bind nonsyntaxin

SNARE proteins, like its cognate R-SNARE and full SNARE complexes<sup>13,19, 40</sup>. Further proving the hypothesis that VPS45 is a stencil for SNARE complex formation.

Even detailed identification of the binding modes and function of a single SM protein has been elusive, let alone finding a common mechanism. Although there does seem to be commonalities between them all e.g. binding to SNARE proteins and being necessary for proper membrane fusion. Knock outs and deletion strains of these proteins have shown various degrees of stalled membrane fusion which suggests a positive role for SM proteins<sup>13, 25, 27, 34</sup>. Knock outs of VPS45 in a mouse model proved to be embryonic lethal at day 7<sup>41</sup>. All of this has led to some confusion in the field, necessitating more careful biophysical, structural, and in vivo investigations.



## VPS45-associated Severe Congenital Neutropenia Mutations

In 2013, natural variants of VPS45 were discovered to be associated with severe congenital neutropenia type 5 (SCN5)<sup>42-46</sup>. SCN is a rare group of diseases characterized by the reduction in circulating neutrophils<sup>47</sup>. SCN is generally caused by one of two factors, neutrophil maturation issues leading to dysfunctional neutrophils in circulation or apoptosis of mature neutrophils such as with ELANE mutants<sup>47</sup>. Each of which causes a decrease of functional neutrophil in circulation, resulting in an inability to fight infection.

SCN5 was linked to three homozygous missense mutations in VPS45 that were isolated from various consanguineous families: E238K, T244N, and P468L<sup>42-46</sup>. All of these mutations are internal and proximal to the binding cavity of VPS45 (**Figure 4**). These mutations are proposed to affect the binding of “closed” conformation of stx16 to VPS45. They are also hypothesized to destabilize the protein itself, which is backed up by clinical data of the patients, where decreased protein levels of VPS45 and its binding partners, stx16 and Rabenosyn 5 (rbsn5) were shown in peripheral blood of patients<sup>42-46</sup>. This destabilization of VPS45 was also observed by our lab when trying to purify the protein from *E. coli* cells (data not shown). SCN5 has a wide variety of presentations including myelofibrosis of the bone marrow, increased peripheral blood apoptosis, neurological symptoms (not fully penetrant), and an overall failure to thrive phenotype, most of which is specific to this type of SCN<sup>42-46</sup>. These patients present with infection early on in life and succumb to the infection if not treated with a bone marrow transplant. Another abnormality of the disease is that it is resistant to normal treatment for SCN, which is G-CSF treatment to promote more neutrophil production in the bone marrow<sup>42-46</sup>. Another lab exploring the mechanism of action for SCN5 found that VPS45 was essential to proper endosome maturation and recycling of cell surface markers, like G-CSF<sup>41</sup>. The neutrophils of the patients appear abnormal with decreased number of granules. These patients, however, are in an almost continuous state of infection, making it hard to tease apart the primary effect of these mutations<sup>42-46</sup>. Therefore, in collaboration with the Newburger lab we created a mouse model to identify the direct effects of VPS45 mutations and to elucidate the underlying dysfunction of SCN5.

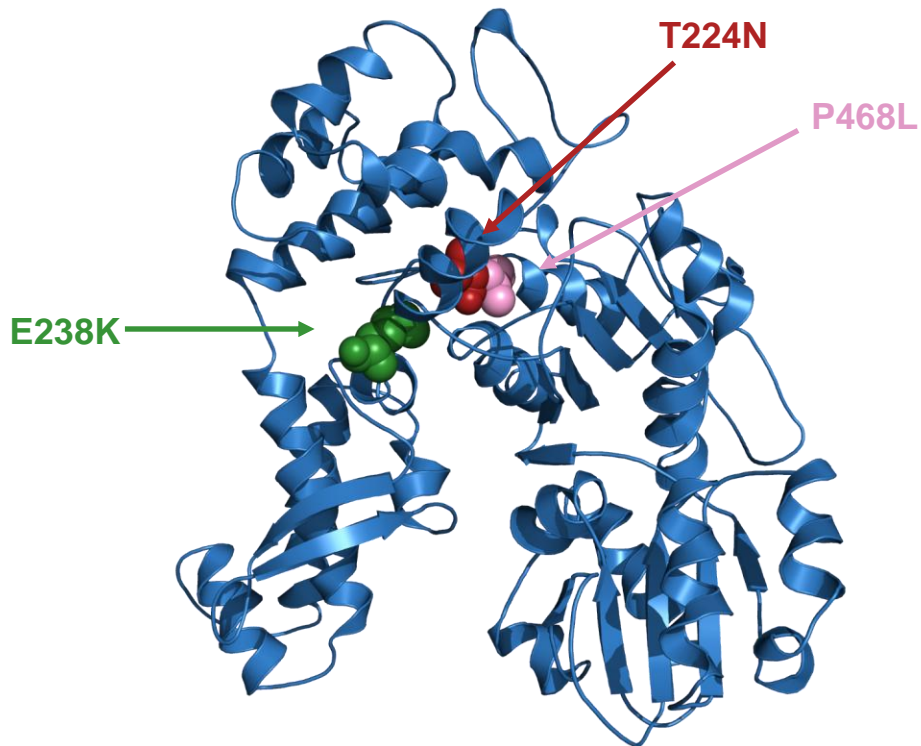
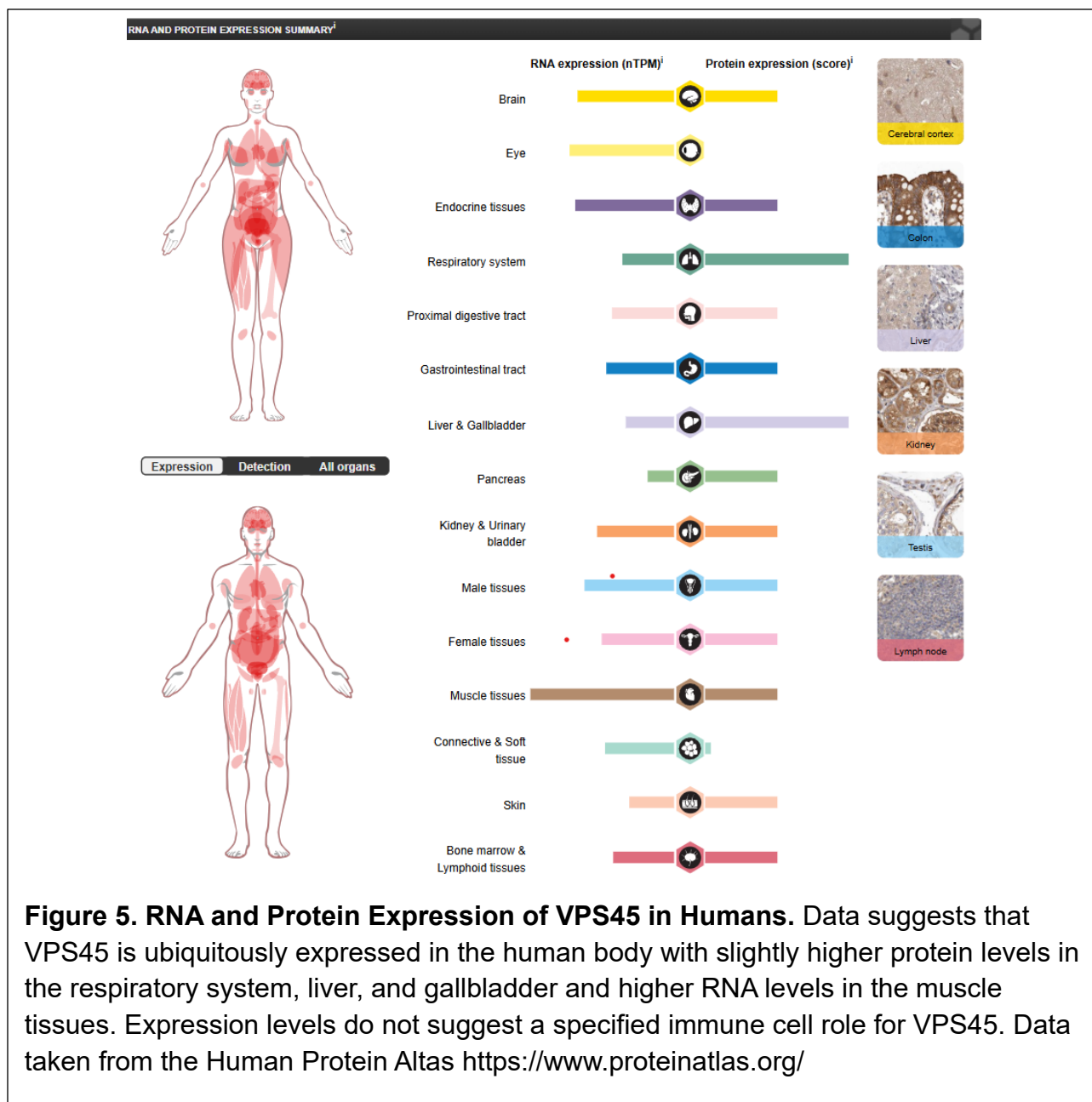


**Figure 4. Model of SCN5-associated VPS45 Mutations.** Mutations are located within the central cavity of VPS45. The central cavity is where VPS45 binds stx16 and proposed to bind SNARE complexes. These mutations are thought to interrupt binding and/or destabilize VPS45 itself. Mutations are T224N (red), E238K (green), and P468L (pink).

### **VPS45 Expression Data.**

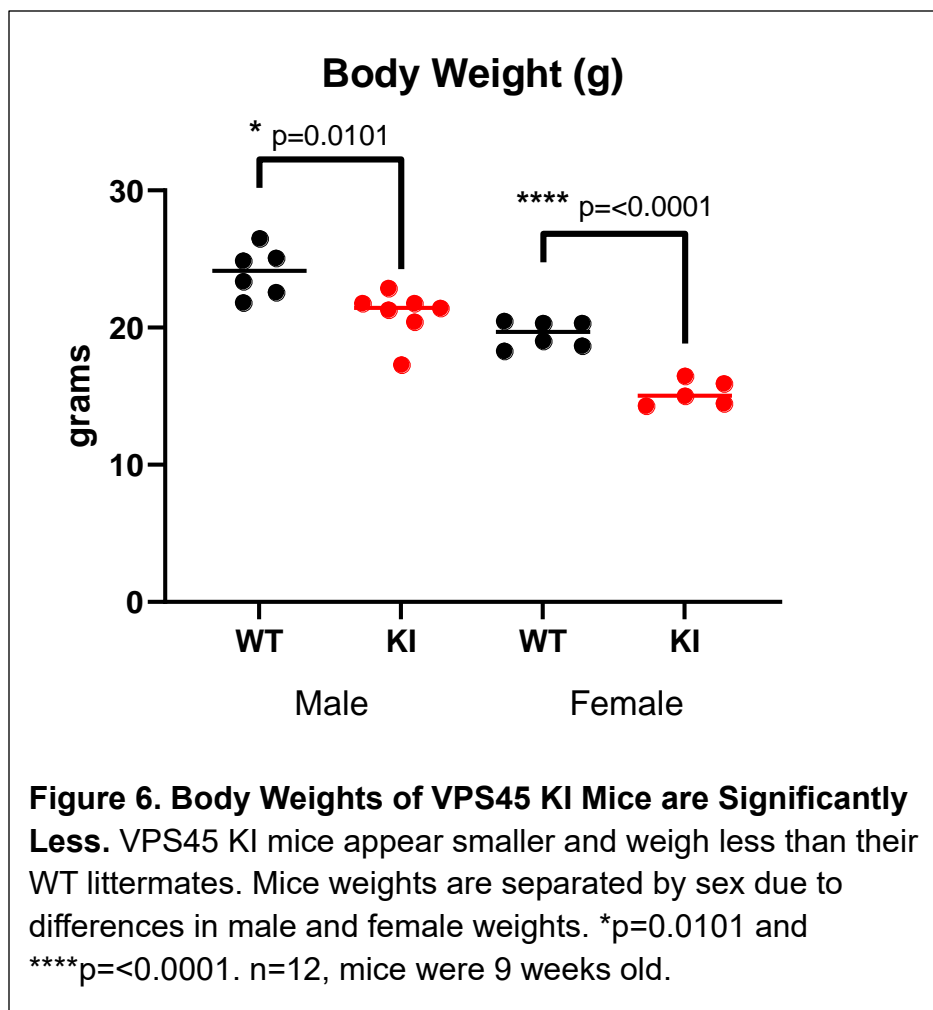
SCN5 is linked to mutations in VPS45, but largely only affects the neutrophils, according to the literature. However, VPS45 is ubiquitously expressed in the body. In order to understand why neutrophils are preferentially affected by the VPS45 mutations, I examined the expression data (**Figure 5**). Examining the protein atlas, there is high expression of VPS45 in the respiratory system, the liver, and the gallbladder. The immune cells do not stand out. So, even with all this data, we are still unaware why the immune system, specifically neutrophils, is being affected in these patients. The SCN5 mouse model sheds more light on this.

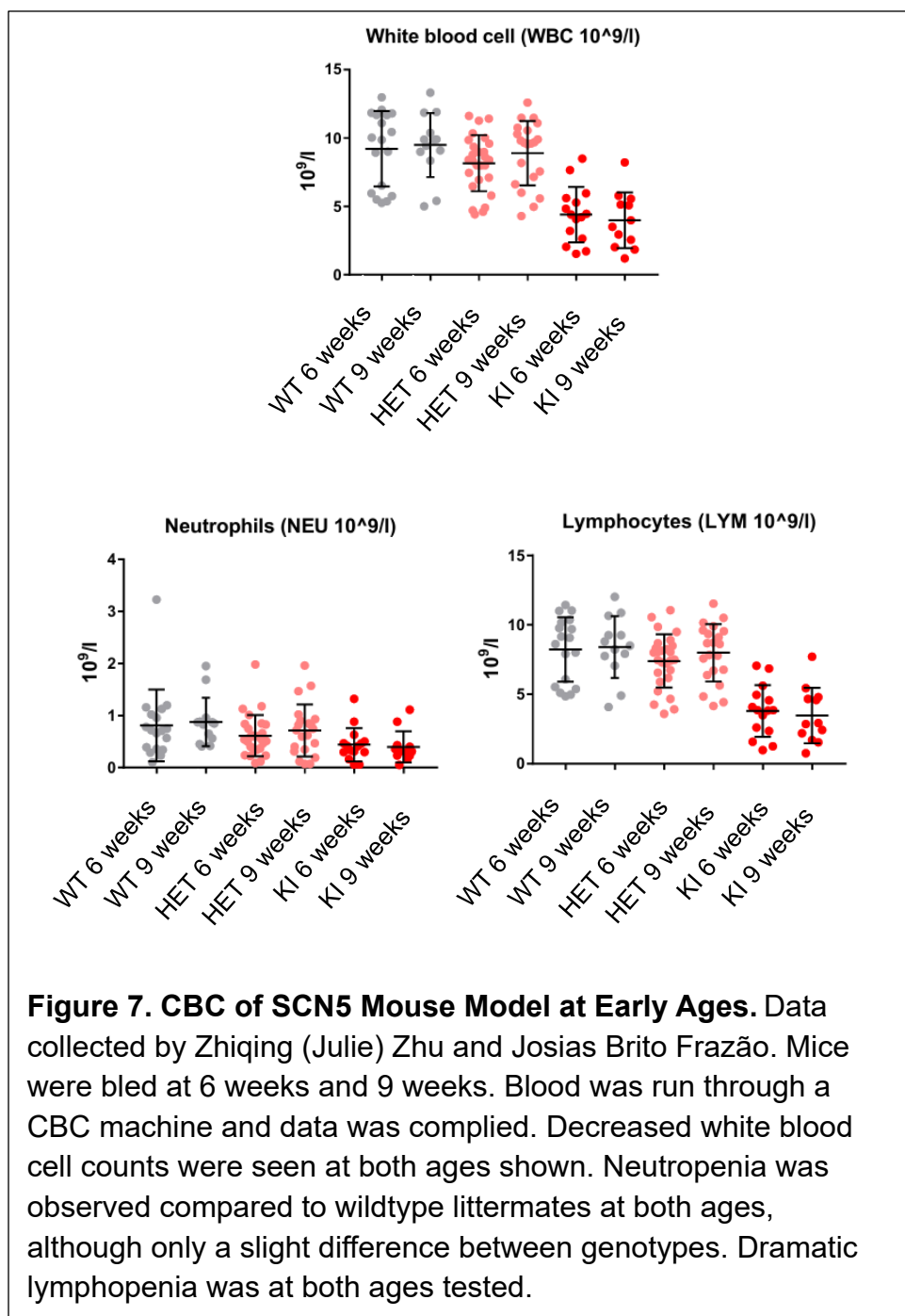


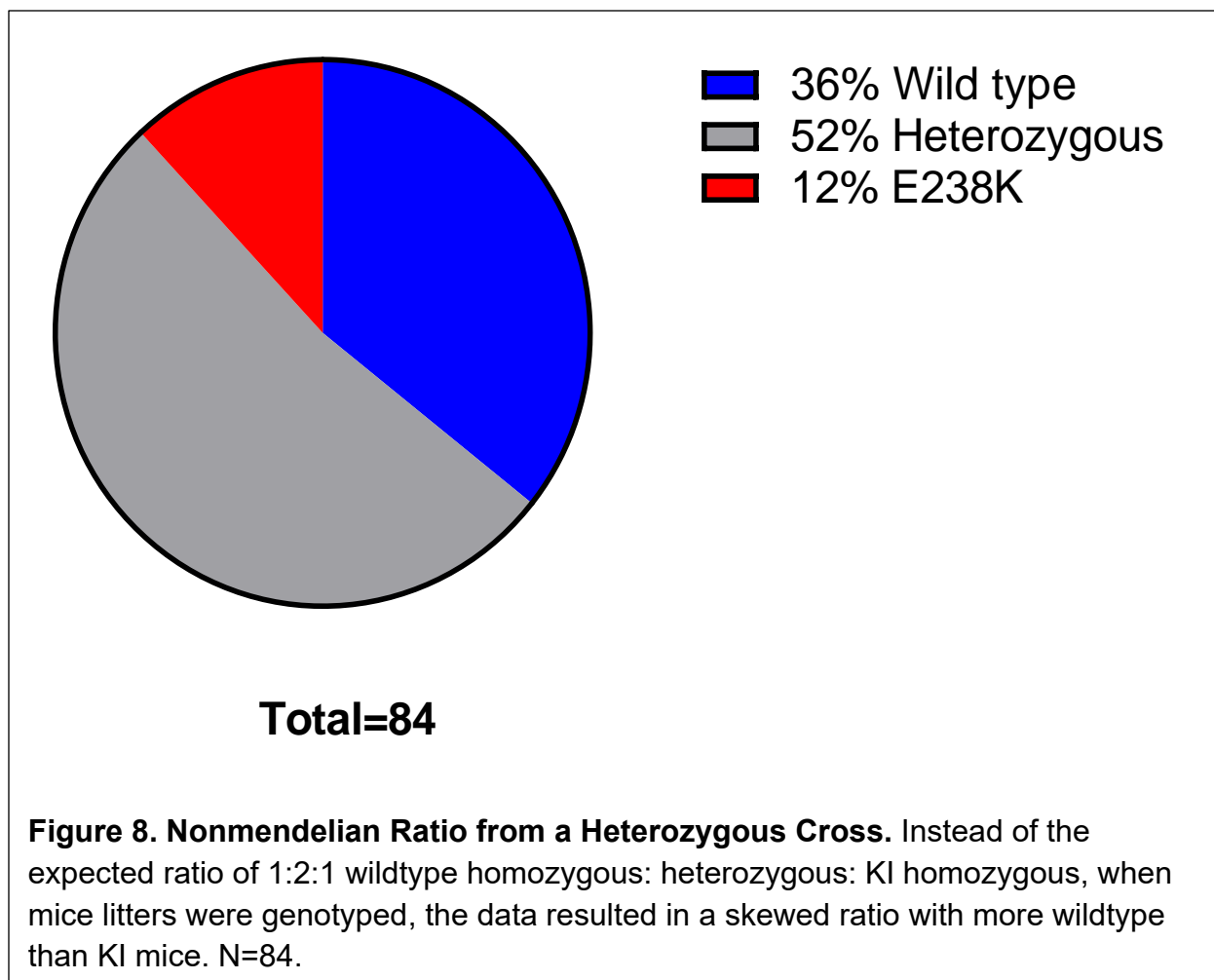
The work presented in my thesis has explored the SCN5 mouse model in order to elucidate the cause of SCN5. My work with the mouse model has largely been to investigate the immune cell landscape and how it differs from that of a wildtype mouse. Interestingly, we found that the VPS45 KI mice have mild neutropenia at early ages and significant T cell lymphopenia. I further probed the T cell landscape to elucidate what subset of T cells are being affected and what state of activation, if any, the T cells were in. I investigated T cell maturation by way of studying the thymus T cell landscape. To preclude any gross morphological defects that could be causing accelerated apoptosis in either the neutrophils or T cells, I used transmission electron microscopy (TEM) of neutrophils and CD8 T cells, the most affected population of cells. This work is just the start, but is pivotal to understanding the presentation of SCN5 mutations and to understanding the importance of VPS45 to immune cell homeostasis.

## CHAPTER II: Creation of the mouse model and initial discoveries.

The creation of the Knock In (KI) mouse model of E238K VPS45 using CRISPR/Cas9 was undertaken by Zhiqing (Julie) Zhu from the Newburger lab with the help of Mike Brodsky and the Transgenic Animal Modeling Core at UMass Chan. One of the first observations was that the VPS45 KI mice were smaller and weighed less than their wild type counterparts (**Figure 6**). Initial characterization of the genotypes was performed using complete blood counts (CBCs) over the lifespan of the mice (**Figure 7**). The Newburger lab discovered mild neutropenia at early ages and pronounced lymphopenia, which I further confirmed using flow cytometry. Additionally, while breeding the mice, we found that the VPS45 KI mice did not appear at Mendelian ratios as one would expect from a heterogeneous cross. Instead, genotyping revealed much lower levels of homozygous mutants than their heterogeneous or wildtype littermates (**Figure 8**). The failure to thrive phenotype aligned with the patient data. The lymphopenia was striking but not entirely unexpected based on the T cell dysfunction that was observed in some of the surviving patients after bone marrow transplants were performed, and a more recent paper describing a new E238K patient<sup>46</sup>.





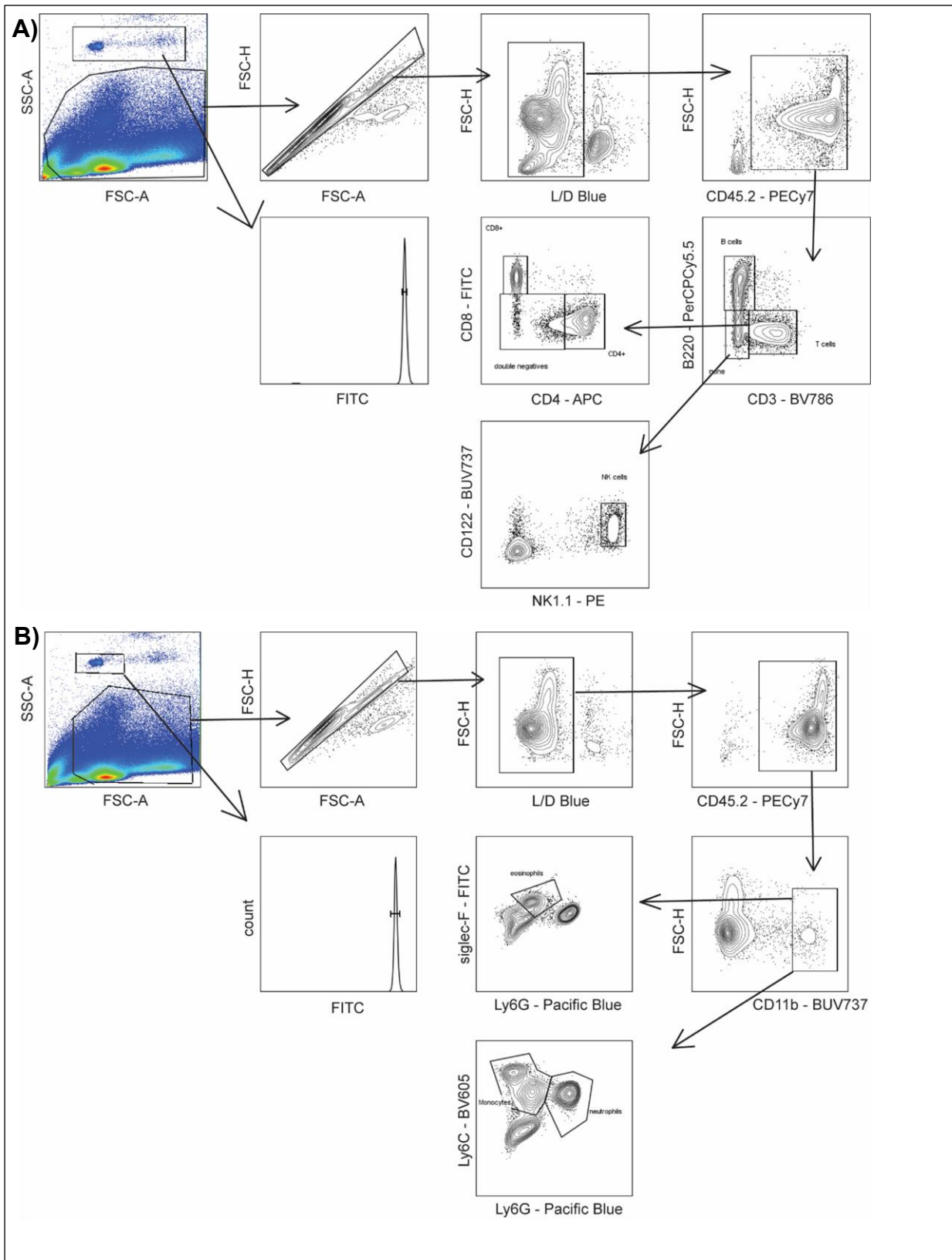


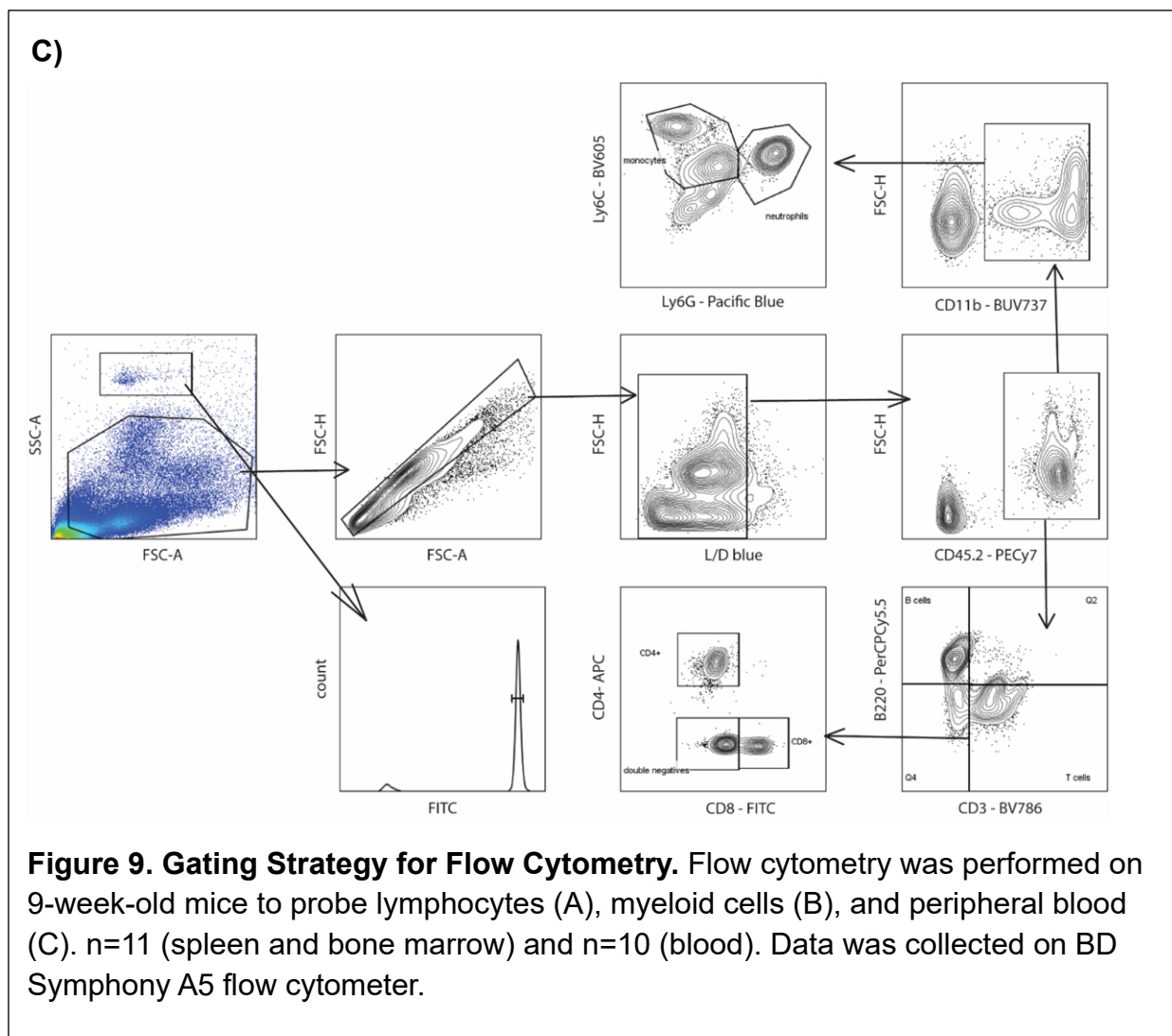
### CHAPTER III: SCN5 phenotype is present in the VPS45 KI mouse model.

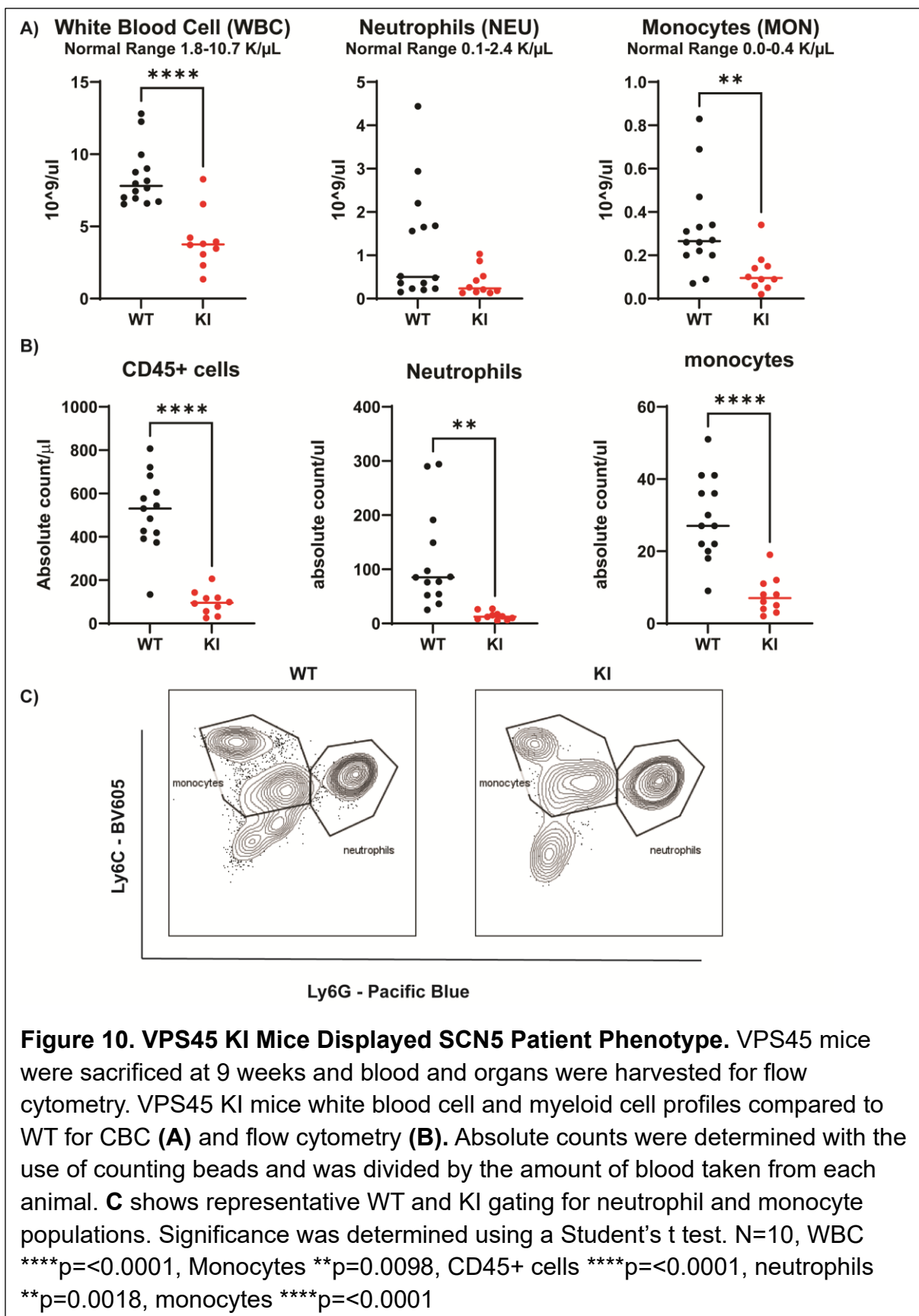
Complete Blood Counts were performed over the lifetime of the mice to determine if neutropenia was present and if it was related to the age of the mice. This data was collected by Zhiqing (Julie) Zhu and Josias Brito Frazão. These data revealed mild neutropenia at early ages and significant lymphopenia at all ages tested. (**Figure 7**). To explore more in-depth the immune cell landscape of VPS45 KI mice and find the root cause of the lymphopenia, I performed flow cytometry on isolated mouse tissues, including blood, spleen, thymus, and bone marrow. Several types of immune cells were identified, including neutrophils, monocytes, eosinophils, T cells, B cells, and NK cells (**Figure 9**).

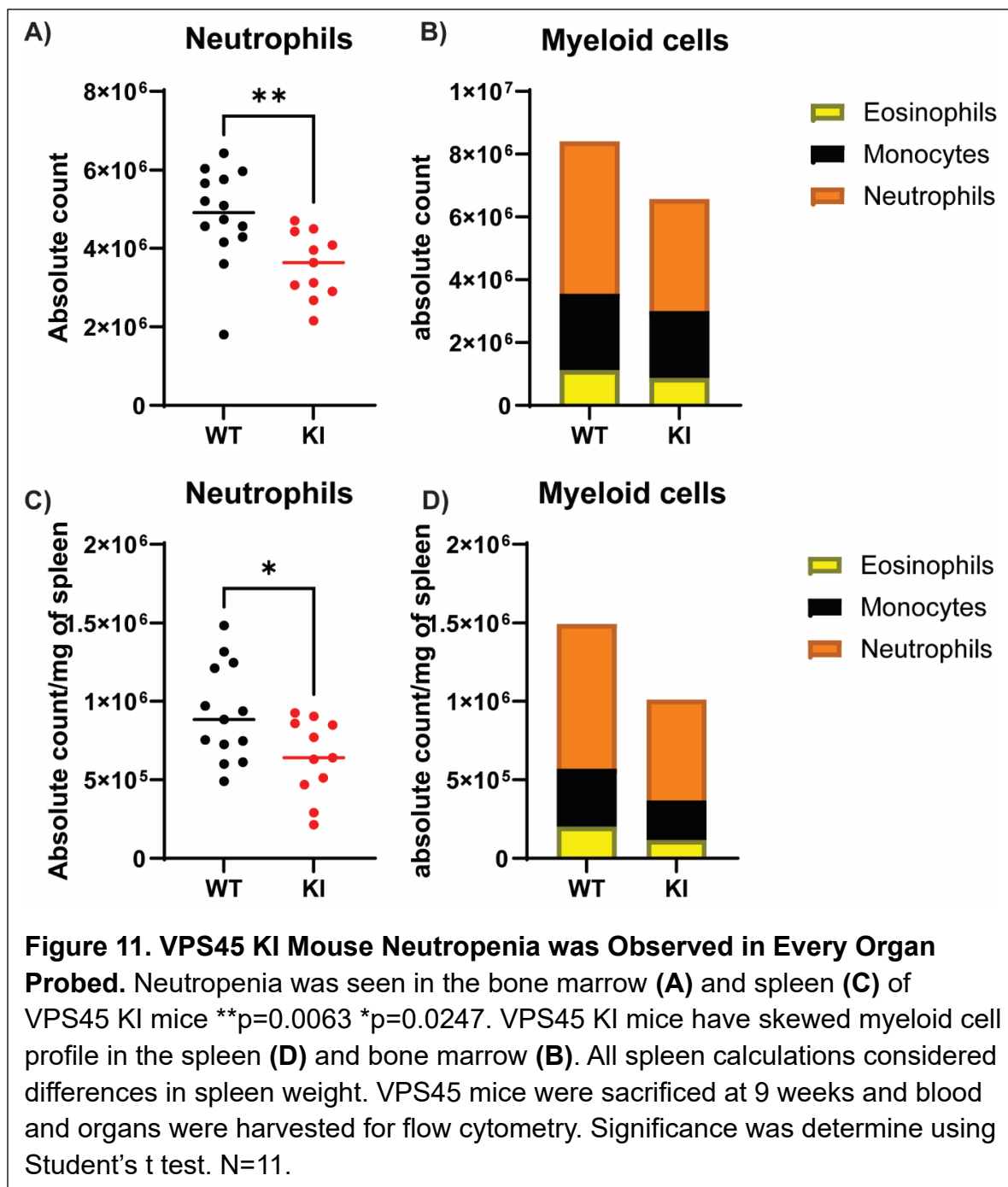
First, I investigated the peripheral blood of the mice at age 9 weeks to align with the age of most pronounced neutropenia, taking CBCs to confirm the initial discoveries. These data generally agreed with the CBC data taken at the 9 week time point of the mice (**Figure 10A & Figure 7**). The flow cytometry data revealed, VPS45 KI mice had fewer white blood cells, as identified by CD45.2 antibody (**Figure 10 B**). Using flow antibodies specific to neutrophils and monocytes, I discovered that VPS45 KI mice had significantly fewer neutrophils, as defined as CD45.2+, CD11b+, Ly6G+, and Ly6C+, and significantly fewer monocytes, as defined as CD45.2+, CD11b+, Ly6G-, and Ly6C+ in the peripheral blood. (**Figure 10 B and C**). Neutropenia was observed in all other organs tested (**Figure 11A and C**). The myeloid profile was slightly abnormal, having lower levels of monocytes, neutrophils, and eosinophils (CD45.2+, CD11b+, and siglecF+) in the VPS45 KI mice spleens compared to their wildtype littermates (**Figure 11 B and D**) (**Figure 12**).

To determine if this neutropenia was a result of aberrant membrane trafficking due to gross morphological differences between the genotypes caused by impaired membrane trafficking, transmission electron microscopy (TEM) of VPS45 KI mouse neutrophils and wildtype littermates was performed. TEM was also used to confirm the results of SCN5 patients, which had revealed decreased granules and possible membrane morphology issues<sup>42-46</sup>. In contrast, the VPS45 KI mouse neutrophils appear WT in appearance and have similar numbers of granules (**Figure 13**). Examining the myeloid cells of our mice, VPS45 KI mice present mainly with neutropenia similar to the disease phenotype, but had overall lower levels of most of the myeloid cells tested compared to their wildtype littermates.









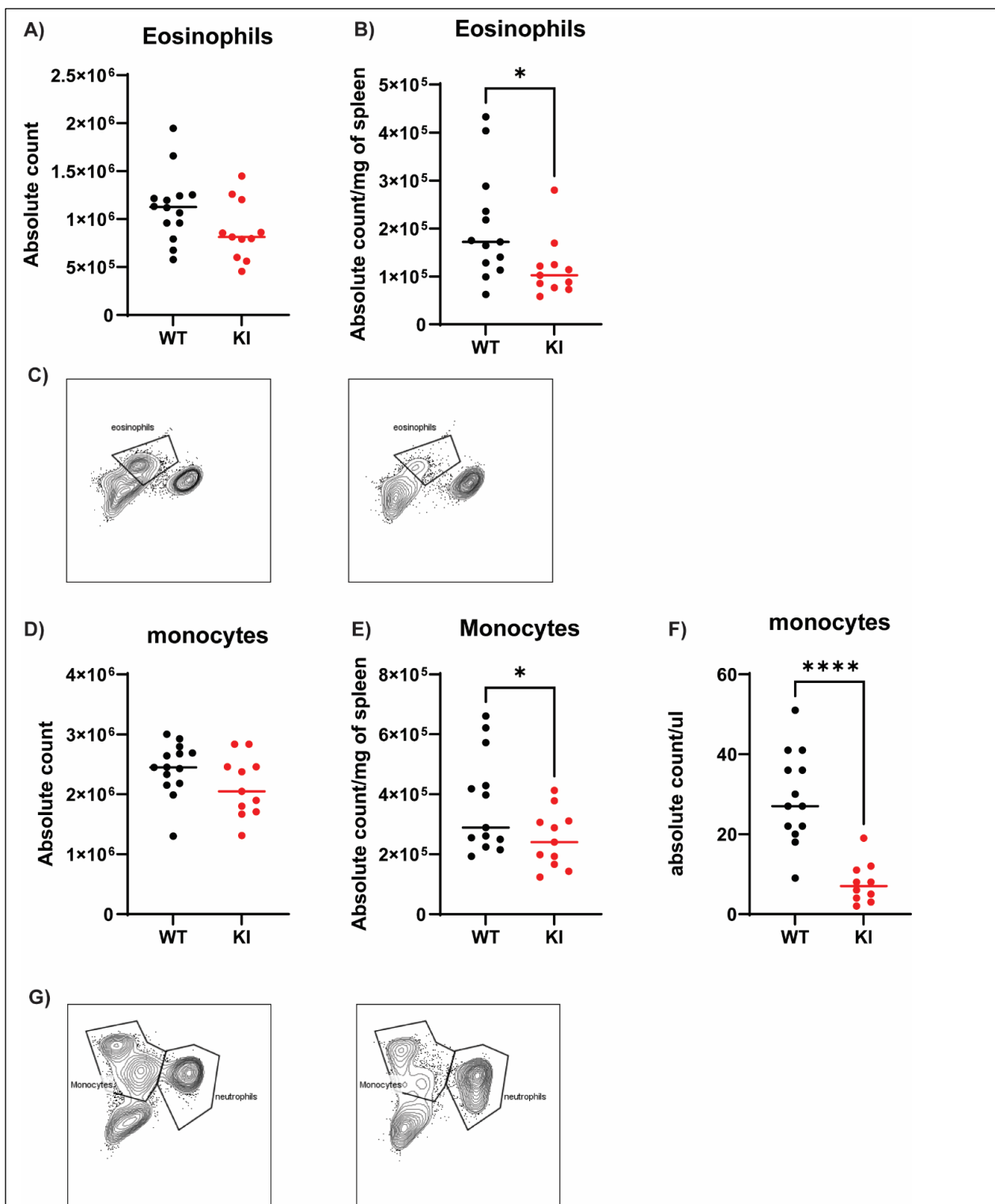
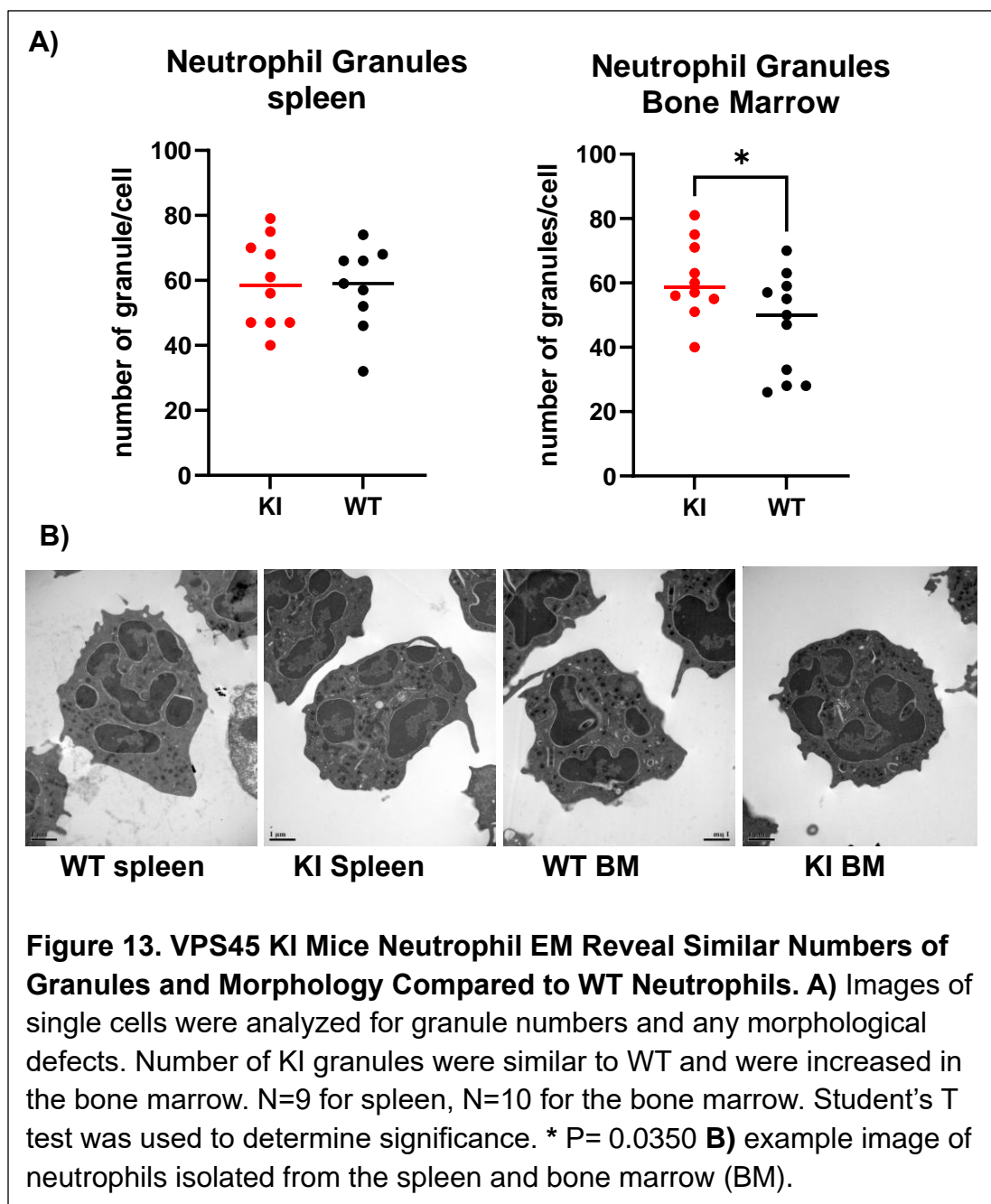


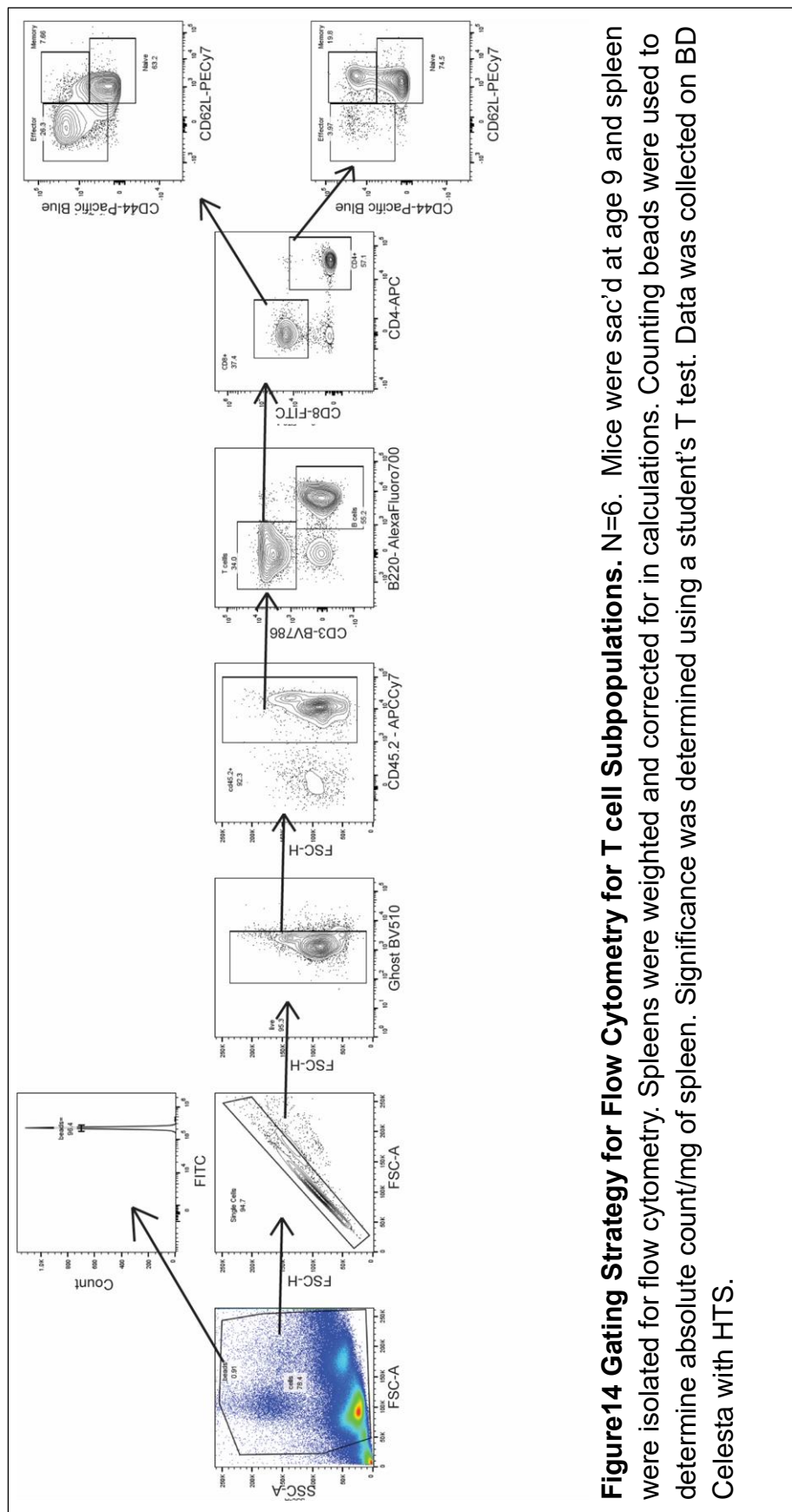
**Figure 12. VPS45 KI Mice had Fewer Myeloid Cells.** VPS45 KI mice and WT littermate appear similar in numbers of eosinophils (A) and monocytes (D) in bone marrow. Eosinophils were fewer in VPS45 KI mice spleens (B) \* $p=0.0368$ . Monocytes were fewer in VPS45 KI mice spleen (E) \* $p=0.0481$  and peripheral blood (F) \*\*\*\* $p<0.0001$ . C and G are representative gating of WT and KI mice in the spleen. Significance was determined using Student's t test. N=11 (spleen and bone marrow) N=10 (blood).



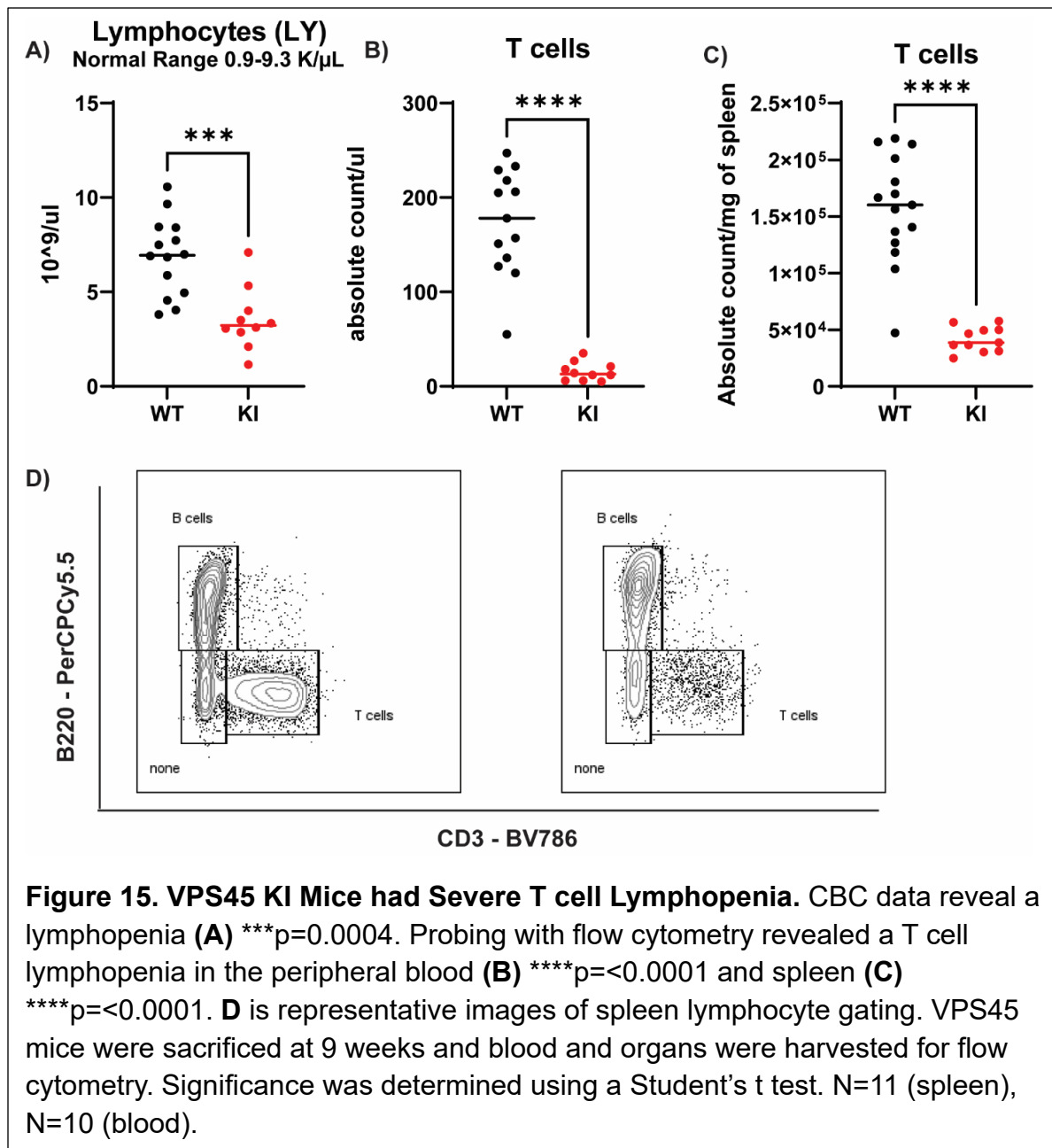
## CHAPTER IV: VPS45 KI mice have T cell lymphopenia.

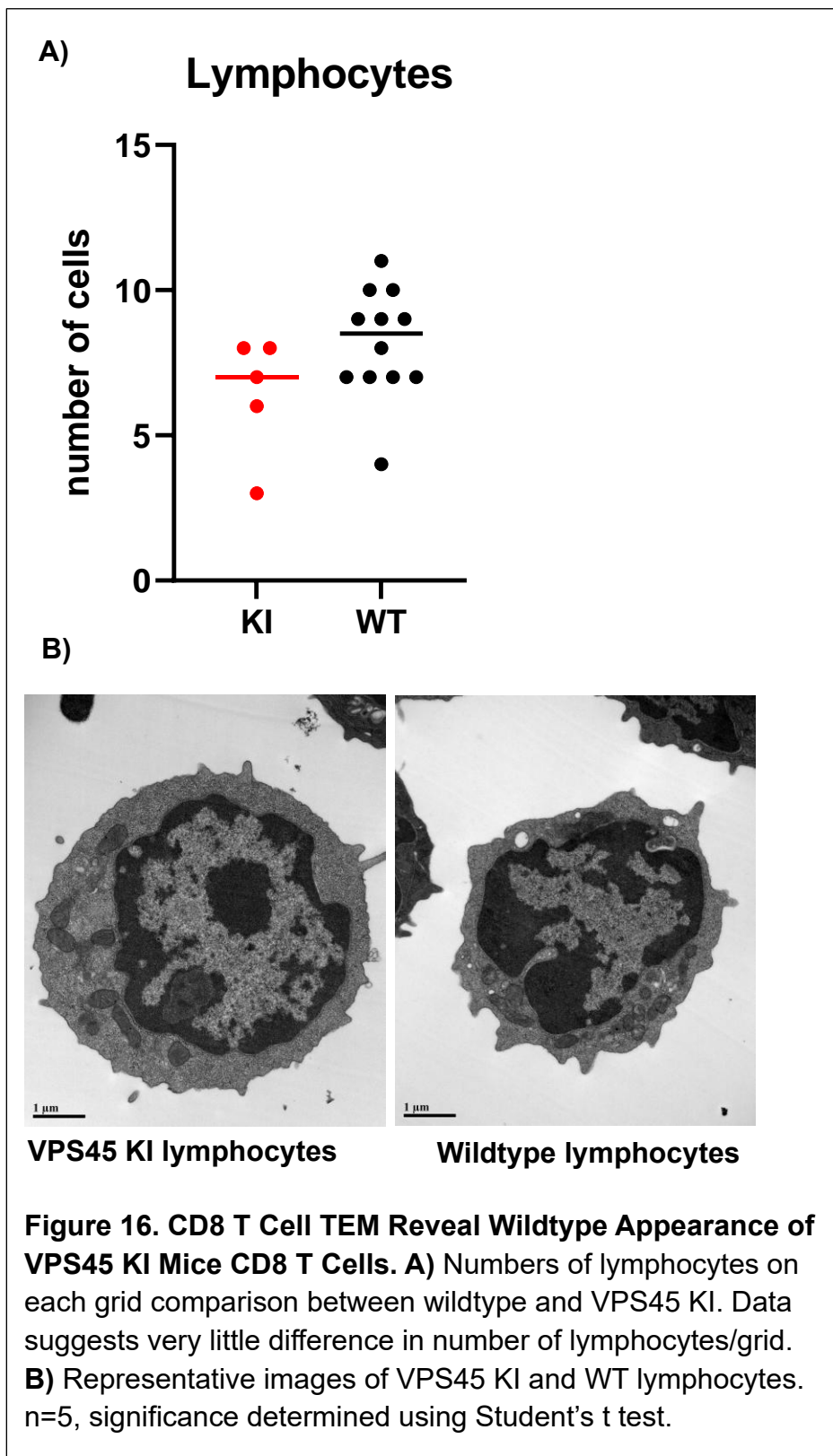
Severe lymphopenia was observed at all ages of the VPS45 KI mice (**Figure 7**). I used flow cytometry to distinguish between the different lymphocyte cells in the spleen and blood to determine the cause of the lymphopenia (**Figure 14 and Figure 9A**). There were significantly fewer T cells in VPS45 KI mice as identified by CD45.2+, CD3+, and B220-. (**Figure 15**). This unexpected dramatic change eluded to a possible link between VPS45 and T cell homeostasis. One possible link between neutrophils and T cells, specifically CD8 T cells, is that they both contain granules. One hypothesis could be that VPS45 may play a pivotal role in granule formation, fusion, or exocytosis. This is an especially relevant hypothesis when taking into account the state of the SCN5 patient neutrophils, who had fewer granules as examined by TEM<sup>42-46</sup>. However, neutrophil and CD8 T cell TEM analysis, where VPS45 KI mice CD8 T cells and neutrophils had wildtype appearance (**Figure 11 and 16**) and flow cytometry data of other granulocyte-containing cells like NK cells, where VPS45 KI mice had more NK cells, disprove this hypothesis (**Figure 17**). The literature also doesn't support this hypothesis with known SNARE proteins in granule formation, fusion, and exocytosis not being proposed to interact with VPS45 or its binding partners<sup>48</sup>.

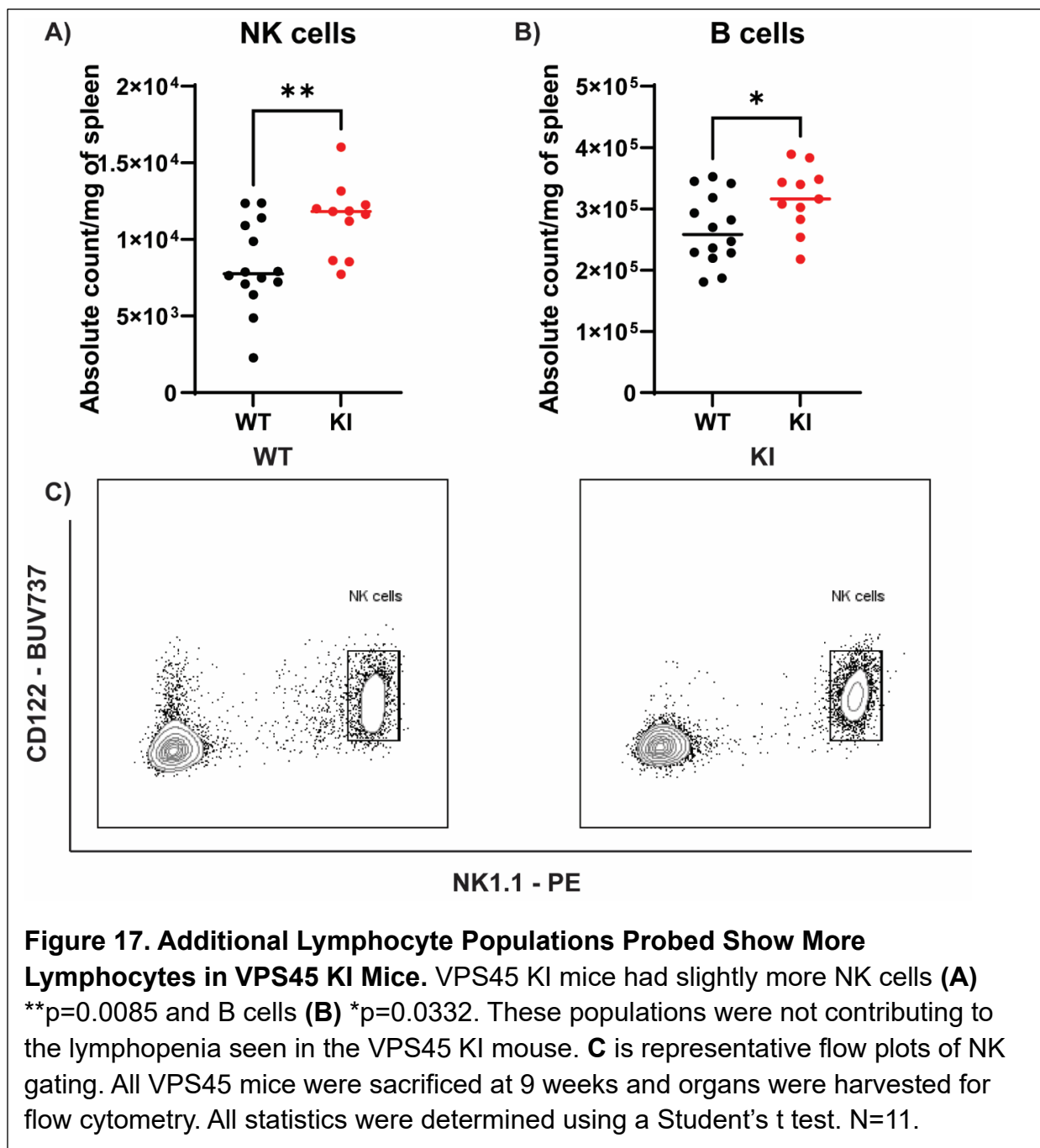
I examined the subpopulations of T cells using flow cytometry. I observed significantly fewer CD4 and CD8 single positive T cells, as identified by CD45.2+, CD3+, B220-, CD4+ CD8- and CD45.2+, CD3+, B220-, CD4-, CD8+, respectively. CD8 T cells were the most significantly decreased (**Figure 18**). Both subpopulations of T cells being affected, indicated a more widely used function or property of T cells is being affected by VPS45 mutations (**Figure 18 A and D**). CD4/CD8 ratio was skewed in the VPS45 KI mouse model, further indicating a holistic T cell phenotype resulting from VPS45 mutations (**Figure 18 B and E**). Using flow cytometry to detect what state the single positive T cells are in VPS45 KI mice, I identified memory (CD45.2+, CD3+, single positive, CD62L+, CD44+) , effector (CD45.2+, CD3+, single positive, CD62L-, CD44+), and naïve (CD45.2+, CD3+, single positive, CD62L+, CD44-) populations. The data revealed that VPS45 KI mice have an increased single positive effector cell population when compared to their WT littermates indicating that the VPS45 KI mice T cells are more activated (**Figure 19**). It is very interesting to observe this increase in expression for the effector population of single positives, as it is opposite of the decreased expression we have observed with most of the other cell markers. This suggests that VPS45 is not involved in recycling of every membrane protein or that the recycling pathway is not as deleteriously affected by VPS45 KI mutations as the previous data suggested. Overall, VPS45 KI mice have fewer T cells, especially CD8, and the single positives have a more activated phenotype.

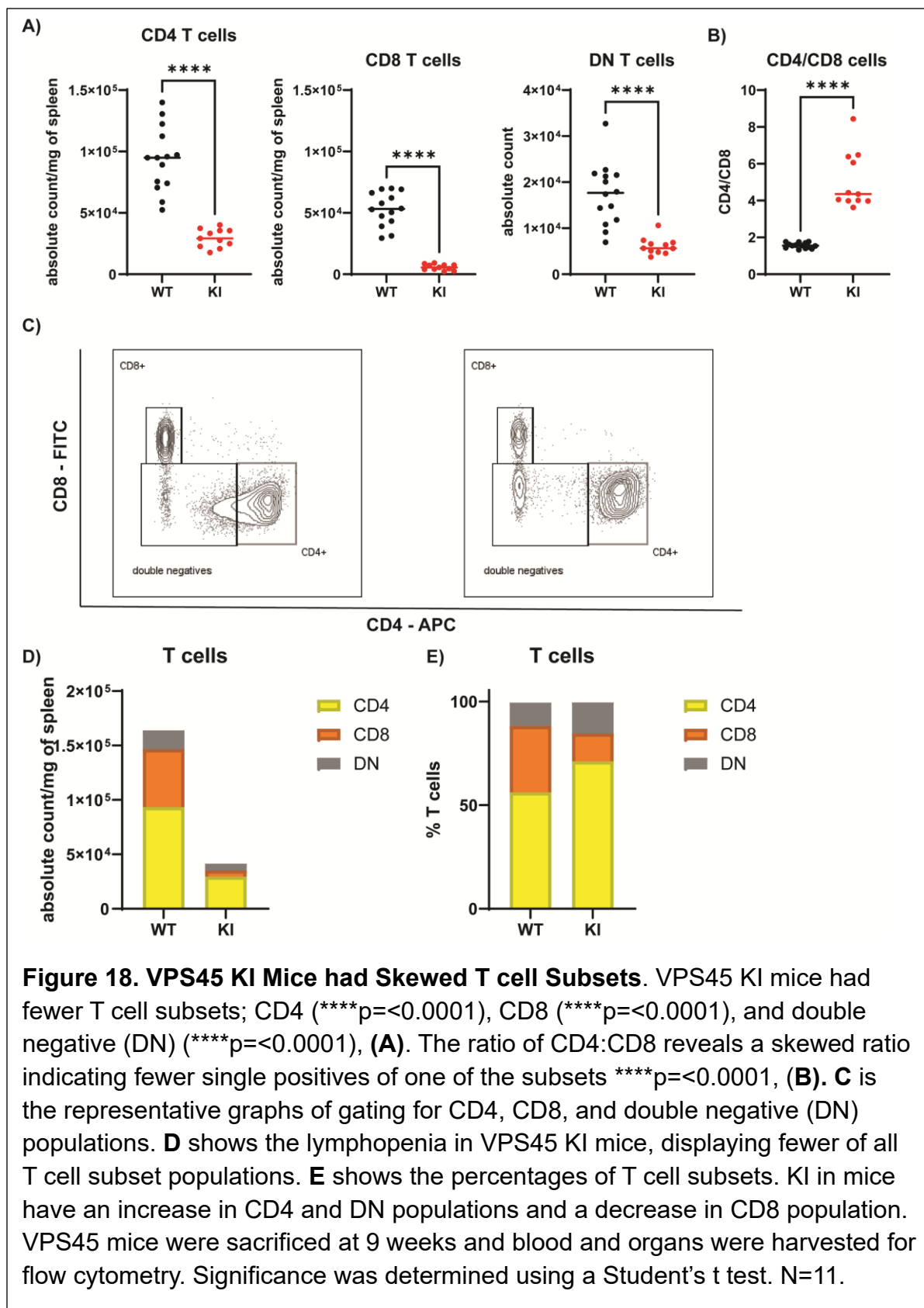


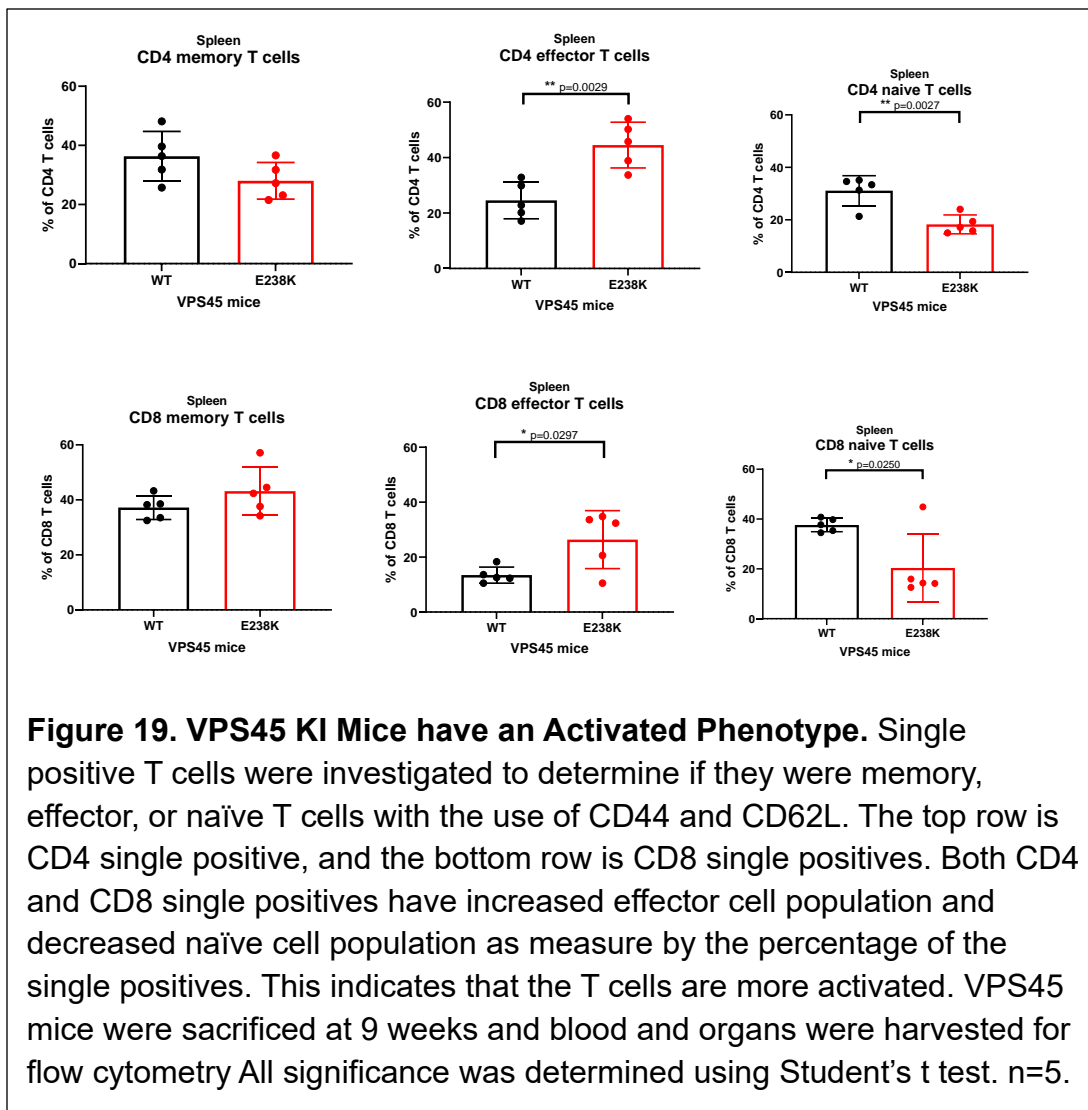
**Figure 14 Gating Strategy for Flow Cytometry for T cell Subpopulations.** N=6. Mice were sac'd at age 9 and spleen were isolated for flow cytometry. Spleens were weighted and corrected for in calculations. Counting beads were used to determine absolute count/mg of spleen. Significance was determined using a student's T test. Data was collected on BD Celesta with HTS.





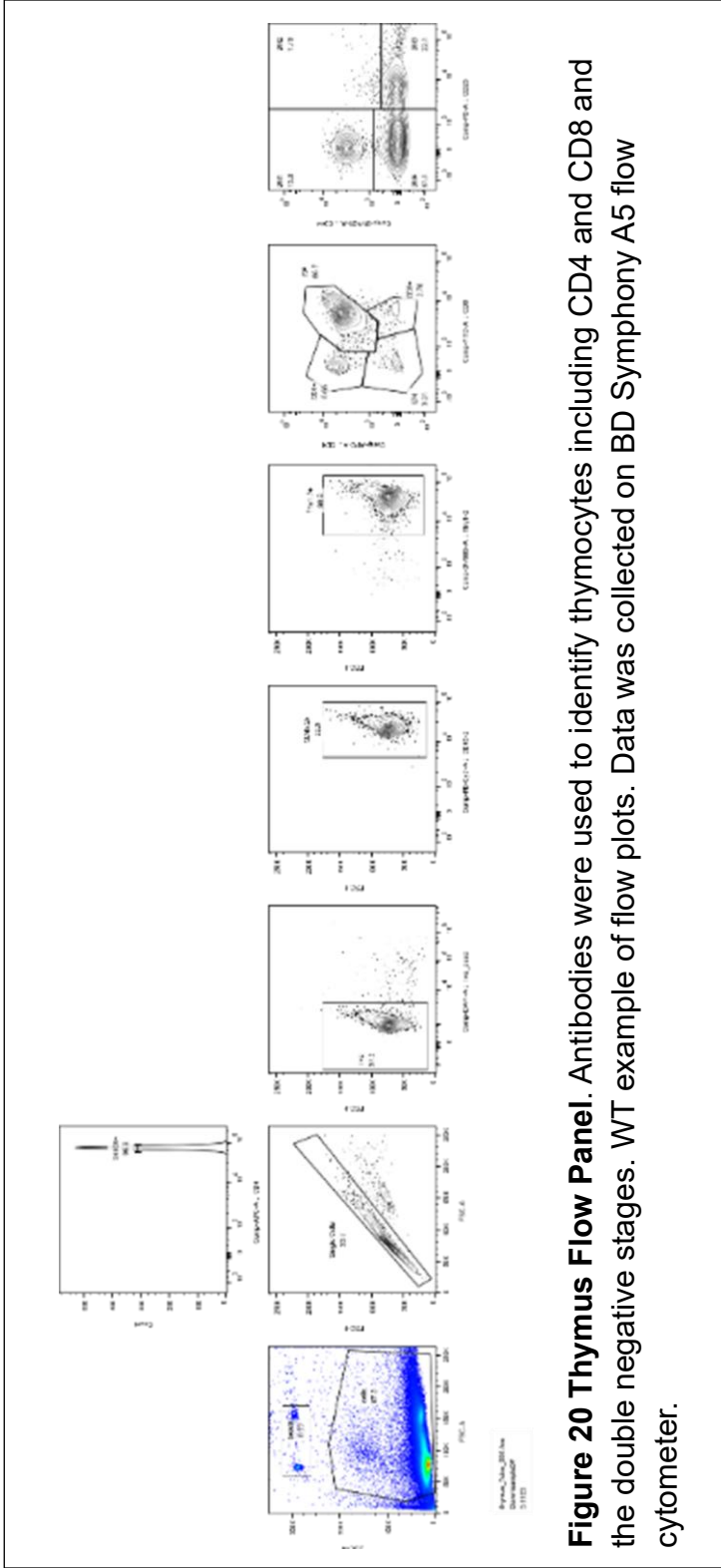


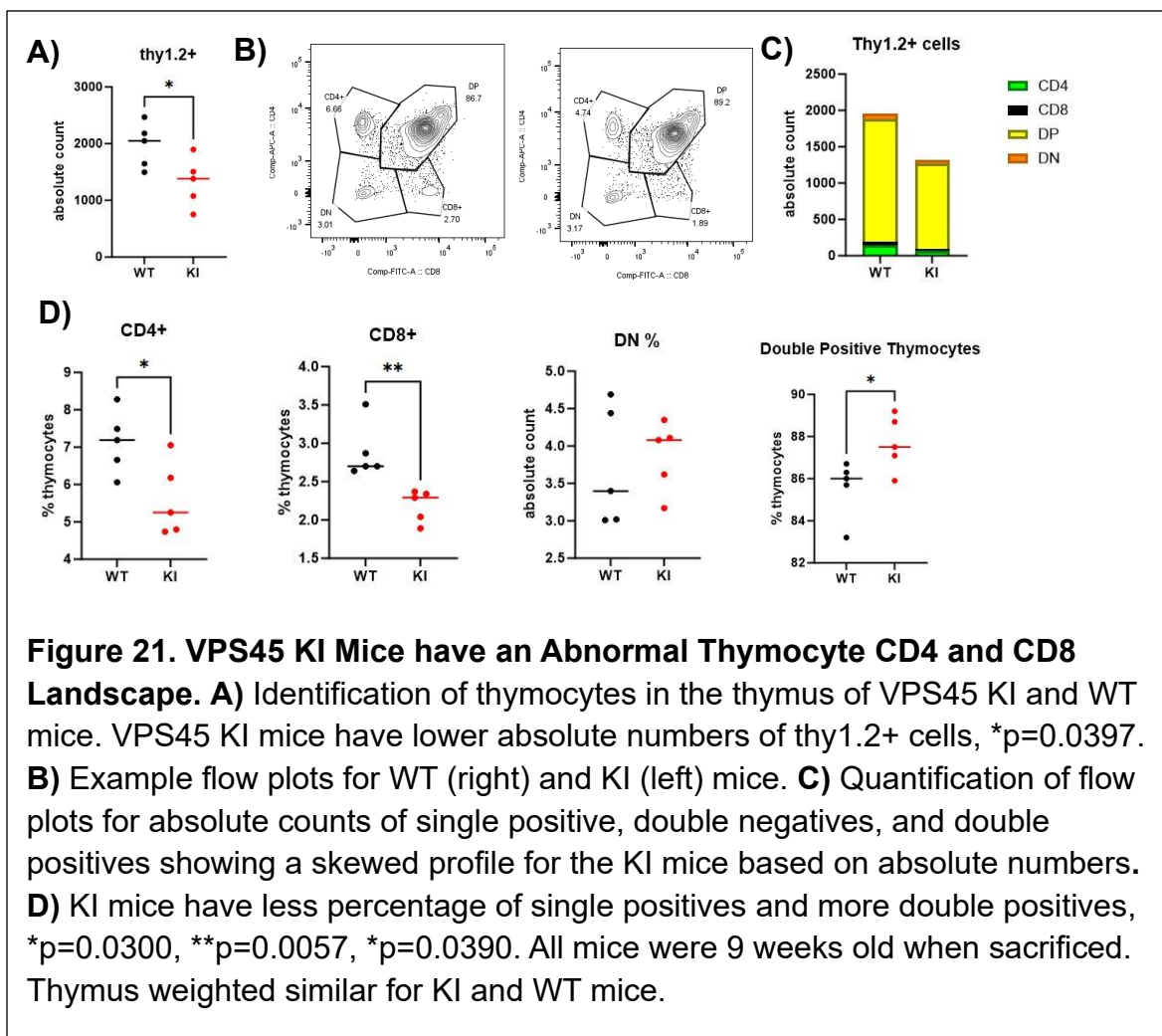


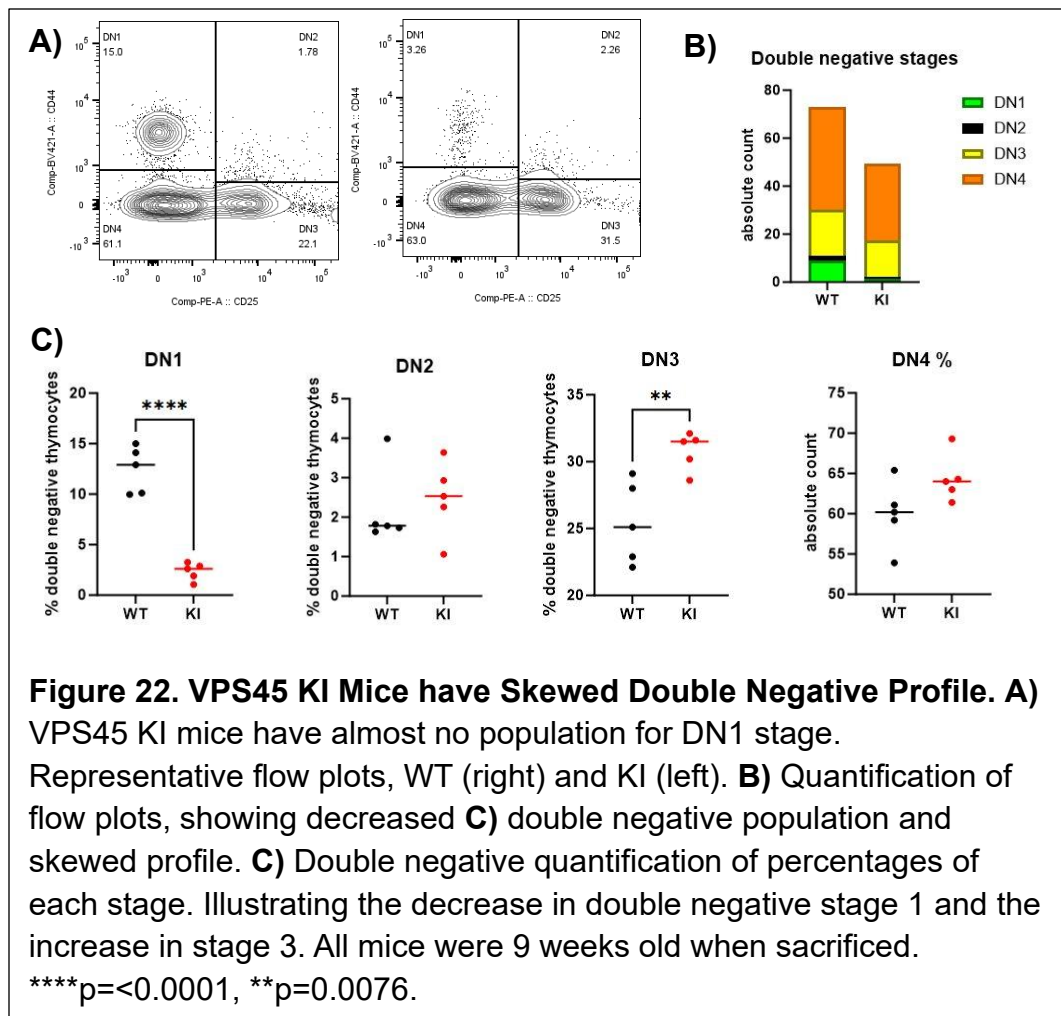


## CHAPTER V: VPS45 KI mice have abnormal thymi.

After discovering that T cell populations were abnormal in the VPS45 KI mice spleens and peripheral blood, I investigated the thymus of the VPS45 KI mice to discover if the T cell lymphopenia started in early development (**Figure 20**). The thymus of mice is where T cells go through early development, going from double negative, based on expression of CD4 and CD8, to double positive to single positive T cells. This is where selection occurs, ensuring that the single positive T cells are reactive to their specific target and react to an appropriate degree<sup>49</sup>. While only modest compared to the differences seen in the blood and the spleen, there was a significant difference in thymocyte numbers between genotypes, with the VPS45 KI mice having fewer (**Figure 21**). I probed the early stages of T cell development in the thymus, including the double negative stages. The double negative stages, broken down into DN1 (CD45.2+, Thy1.2+, CD4-, CD8-, CD44+, CD25-), DN2 (CD45.2+, Thy1.2+, CD4-, CD8-, CD44+ CD25+), DN3 (CD45.2+, Thy1.2+, CD4-, CD8-, CD44-, CD25+), and DN4 (CD45.2+, Thy1.2+, CD4-, CD8-, CD44-, CD25-) and are identified by the lack of CD8 and CD4 receptors. This is a critical stage of T cell development where the T cell receptor gene is rearranged and where selection starts to occur<sup>49</sup>. The VPS45 KI mice have a decreased proportion of double negative cells in the first stage of double negative development, DN1 (**Figure 22**). This difference was striking and could potentially indicate a migration defect in the VPS45 KI mice. With all of this data pointing to a T cell defect in the VPS45 KI mice, it is still hard to tease apart what is a result of defects in the T cell or possible defects with the tissues that the T cell develop in. Myelofibrosis of the bone marrow could make it more difficult for the T cell to migrate out of the bone marrow and get to the thymus, there could be issues with selection in thymus itself, or all of this could be due to membrane protein recycling or another undiscovered defect of the actual T cell. In other words, based on the expression of VPS45 being ubiquitous (**Figure 5**), I can not determine if the differences between genotypes is cell intrinsic or extrinsic.

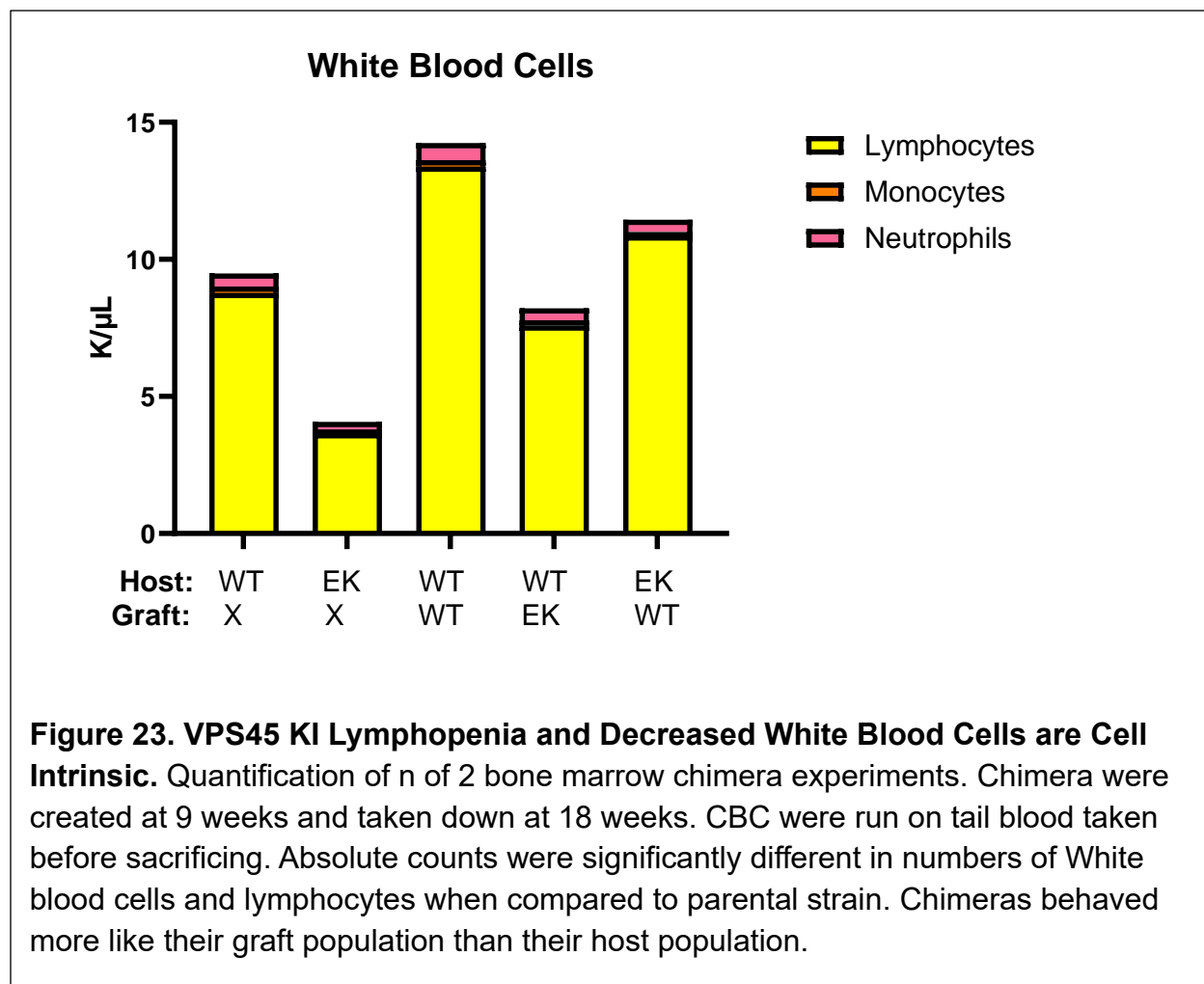






## **CHAPTER VI: Preliminary data suggests T cell lymphopenia is intrinsic.**

In order to discover if the T cell or other phenotypes observed in the VPS45 KI mice were cell intrinsic or extrinsic, I performed bone marrow chimera experiments with the Rothstein lab. In short, mice were irradiated with 750 rads, allowed to recover then were injected via the tail vein with the bone marrow of another genotype. The chimera mice were either; control WT host with WT graft, experimental KI host with WT graft or experimental WT host with KI graft. The preliminary data presented below is from two separate experiments. CBC data collected at the time of sacrifice. Flow cytometry data was lacking as many of the KI mice with WT graft did not survive the experiment. More experimentation is needed to be confident in this data set. However, this preliminary experiment suggested that the lymphopenia was intrinsic to the T cell itself when compared to parental strains (**Figure 23**).



## CHAPTER VII: Discussion

This thesis has revealed in-depth immune cell profiling in the VPS45 KI mice. In this study, VPS45 KI mice were followed at early ages with CBCs to elucidate if the mice presented the same phenotype as SCN5 patients. This data indicated that while neutropenia is the primary phenotype in SCN5 patients, lymphopenia is prominent in the VPS45 KI mice. I used flow cytometry to confirm these findings and discovered that the lymphopenia observed in the CBC data was caused by T cell lymphopenia, specifically CD8 T cells. Flow cytometry revealed decreased myeloid cell numbers for the VPS45 KI mice compared to their wildtype littermates. For almost all the cell types identified in this study, VPS45 KI mice have at least a slight decrease in number. This could be a result of the failure to thrive phenotype. However, work done on VPS45 protein have revealed that recycling of certain membrane proteins is delayed when VPS45 is absent<sup>50, 51</sup>. Additionally, the Klein lab which has done some characterization of SCN5 mutations and VPS45 deletions in cell lines and mouse model, observed impaired recycling of cell surface proteins, including G-CSF receptor<sup>41</sup>. Impaired recycling of cell surface proteins could account for the overall decrease in immune cells, as identified by their cell surface proteins. However, it does not account for the dramatic and significant effect on T cells seen in this publication. It also doesn't account for the increase in effector cell populations of single positive T cells and the other lymphocytes. The proteins chosen for cell identification may have various degrees of recycling, resulting in differing levels of decreased cell surface proteins. More experimentation is needed to answer this question.

To investigate where the T cell lymphopenia was originating from, I investigated the VPS45 KI mice's thymi. Flow cytometry indicated that VPS45 KI mice have abnormal thymic T cell proportions. The greatest difference between genotypes was observed in the DN1 of double negative development. This could be a product of improper or irregular migration from the bone marrow to the thymus. This again could be a product of impaired recycling in the VPS45 KI mice. The bone marrow of the SCN5 patients showed various degrees of myelofibrosis, while not observed to the same degree in the VPS45 KI mice; this could have an effect on migration out of the bone marrow to the thymus. Although this is likely not the case based on the bone marrow chimera experiments, which showed lymphopenia in the WT host KI graft mice. Further chimera experiments would need to be performed using flow cytometry and migration experiments to elucidate the thymus phenotype.

The Human Protein Atlas explored the expression of VPS45 in various tissues. This data revealed that VPS45 is ubiquitously expressed in the body with no specific affinity for neutrophils or T cells. Regardless of this, we observed that these VPS45 mutations have caused neutropenia in patients and T cell lymphopenia in mice. Why could this be? Originally, we had hypothesized that the sensitivity of the cell type, neutrophils, and their higher propensity for apoptosis, but with this mouse model data, that calls that hypothesis into question. However, there could be inherent differences between mouse neutrophils and human neutrophils that could account for the mild presentation in VPS45 KI mice, this has not been fully explored. One new case of SCN5 parallels the data we have gathered with the VPS45 KI mouse model, with the patient being

described as not only neutropenic but also T cell and NK cell lymphopenic<sup>46</sup>. This hypothesis lends some credit to the original hypothesis that VPS45 is playing a role in granule formation and/or exocytosis. However, this directly contradicts some of the data presented in this thesis, including the increase in the number of NK cells observed in the spleen and the wildtype appearance of the neutrophils and CD8 T cells. More detailed analysis of the function of the VPS45 KI mice T cells and NK cells would need to be done to compare these data sets to each other.

Literature has shown a link between syntaxins and granule-containing cells. One group looking into the effects of syntaxin 11 on the immune system, which is linked to diseases like FHL-4, which affects NK cells in patients, discovered that when stx11 null mice were generated, there were NK cell, T cell, and neutrophil effects<sup>52</sup>. It is known that stx11 is necessary for lytic granule exocytosis<sup>48</sup>. The paper describes the null mice as having defective exocytosis of granules in neutrophils and impaired cytotoxicity in NK cells and CD8 T cells<sup>52</sup>. While stx11 has no links to VPS45, its binding partners, stx16, or rbsn5, it is one of the few papers that explore the relationship between syntaxins and immune cells. It also showcases the selective nature of knock out of syntaxins for the immune cells. Why this may be is not fully understood. However, we can use this information to view our phenotype. It is possible that having decreased levels of stx16, which was identified in the patient's peripheral blood and the tissues tested in the VPS45 KI mice, could selectively affect the granule-containing immune cells as well. Even though there is no link between VPS45 or its binding partners, stx16, or rbsn5, and granule formation or granule exocytosis, unlike stx11. Decreased stx expression may be enough to impair the delicate nature of degranulation, or the process of degranulation requires proper membrane trafficking.

Another paper looking at the link between syntaxin 4 and immune cells, found that stx4 is necessary for recycling of membrane proteins necessary for proper exocytosis of lytic granules<sup>53</sup>. This recycling process helps to deposit stx11 from recycling endosomes onto the plasma membrane to interact with other SNARE proteins and exocytosis the cargo in lytic granules at the immune synapse. The Klein lab and others have proven that VPS45 is needed for proper recycling of certain membrane proteins<sup>41</sup>. This could also be true of internal membrane proteins, like SNARE proteins needed for proper exocytosis of granules. To explore this hypothesis, we would need to do cell-based assays looking at the localization of SNARE proteins important for the exocytosis of granules. And degranulation assays, like measuring CD107a levels on the surface of the cell. This data would help to figure out why our CD8 T cells, NK cells, and neutrophils could be preferentially affected. However, this would contradict the patient data where the neutrophils have decreased granule numbers, although this could be an artifact of being in a constantly infectious environment. VPS45 KI mice would help to shed light on this dilemma.

In summary, my results demonstrate that VPS45 is necessary for a proper immune cell landscape. SCN5 mutations in mice cause mild neutropenia, T cell lymphopenia, especially CD8 T cells, and decreased numbers of almost all the immune cells tested. Whether this is a product of improper recycling, decreased VPS45 and binding partners, or a dysfunctional VPS45, needs further cell-based assays to determine. This study

does show the importance of membrane trafficking and illustrates what can happen when even just one step in the process is altered.

## Methods and materials

### Mouse tissue processing

VPS45 Knock In homozygous missense E238K mice were created using CRISPR/Cas9 in a C57BL/6 parental strain by Zhiqing (Julie) Zhu with the help of Mike Brodsky and the Transgenic Animal Modeling Core at UMass Chan. VPS45 KI mice and their WT littermates were used between 6-9 weeks and maintained in clean conditions at the University of Massachusetts Chan Medical School. All experiments were performed in compliance with national and institutional guidelines. Complete blood counts and peripheral blood samples were collected as follows. Mice were bled via their tail vein. In short, mice were warmed up for 5-7 minutes. Their tails were cut, and 150-650 $\mu$ l of blood was collected. CBCs were run immediately. After CBCs, blood samples then underwent red blood cell lysis using Red Blood Cell Lysing Buffer Hybri-Max (Sigma-Aldrich #R7757). Blood was incubated with 2.5 mL of lysing buffer for 5 minutes. This was done twice. Then blood was incubated with an additional 1 ml of lysing buffer for 1 min. In between each incubation, PBS was added to dilute the lysing buffer, and cells were pelleted (400xg, 5 mins, 4 °C). After RBC lysis, blood samples were then resuspended in 1 mL Flow Buffer (PBS, 5% FBS, 5 mM EDTA) with Mouse BD Fc Block (BD Biosciences #55341, 1 $\mu$ g/100 $\mu$ l). Blood single cell suspensions were then stored on ice while processing other organs.

Mouse weights were taken one day prior to sacrificing to save time on the day of. On the day of, mice were sacrificed in accordance with our protocols, using the double kill method of CO<sub>2</sub> and cervical dislocation. Spleen and thymus were removed immediately after sacrificing and were weighed and recorded. The femur and tibia of the mice were removed to isolate bone marrow. All organs and bones were stored in Isolation Media (RPMI buffer with 10% FBS and 1x penicillin and streptomycin) while additional mice were sacrificed and organs isolated. The spleen and thymus cells were isolated from the organs via mechanical force. The femur and tibia bone marrow cells were isolated via flushing the bones with Isolation Media. Spleen, thymus, and bone marrow single cell suspensions were stored in Isolation Media on ice. All samples were pelleted (400xg, 5mins, 4°C). For the spleen and bone marrow samples, red blood cell lysis was performed using Red Blood Cell Lysing Buffer Hybri-Max. Cells were incubated with 1 ml of lysis buffer for 1 min, washed, and pelleted. Cells were resuspended in 1 mL Flow Buffer with Fc block and placed on ice. All samples, including blood, were then counted with a 1:1 mixture of 0.4% trypan blue (Sigma-Aldrich #93595). Spleen, thymus, and bone marrow samples were diluted for counting 1:100 with PBS.

### Flow Staining

After counting isolated cell suspensions, 4x10<sup>6</sup> cells were taken from each single cell suspension and plated accordingly on a 96-well plate. A 200 $\mu$ l sample was heated to 65°C for 5 mins as a dead control and added to the 96-well plate. The cells were then pelleted (400xg, 5mins, 4 °C) and the correct antibody mixture was added to each sample for staining. The cells were incubated at 4 °C for 30 minutes in the dark with antibody solutions. Cells were then pelleted (400xg, 5 mins, 4 °C) and washed three

times with Flow Buffer. Cells were then fixed in 50 $\mu$ l of FluoroFix Buffer (Biolegend #422101) for 30 mins at room temperature in the dark. After incubation, 100 $\mu$ l of Flow Buffer was added to each well, and samples were pelleted (400xg, 5 mins, 4 °C) and resuspended in 200 $\mu$ l of Flow Buffer. Samples were stored at 4°C in the dark for 1 day. Once transferred to tubes for flow cytometry analysis, 10 $\mu$ l of counting beads were added to each sample. Samples were then run on the BD Symphony A5 flow cytometer at the Flow Core Facility, except the lymphocyte activation panel, which was run on the BD Celesta with HTS. Data was collected and processed through BD FlowJo (see figures for gating strategy). Absolute counts were determined using the counting beads. Data was graphed using Dotmatics GraphPad Prism. All significance was determined using a Student's t-test. Spleen samples were normalized to spleen weight to account for differences in spleen weight between the VPS45 KI and WT mice. All blood samples were normalized using the amount of blood taken from each animal to account for the difference in volume collected.

### Antibody mixture

Blood samples: B220-PerCPCy5.5 (Biolegend #103235, 5:100), CD8-FITC (Biolegend #100705, 1:500), CD3-BV786 (BD sciences #564010, 3:100), Ly6C-BV605 (Biolegend #128035, 1:25), Ly6G-Pacific blue (Biolegend #127611, 1:100), CD4-APC (Biolegend 100411, 1:200), CD11b-BUV737 (BD sciences #612800, 1:200), L/D blue (Invitrogen #L23105, 1:50), CD45.2-PECy7 (Biolegend 109830, 5:100), G-CSF receptor-PE (Abcam #AB233582, 1:5) and PE isotype (BD sciences #550617, 1:100). Myeloid samples: siglec-F-FITC (Biolegend #155504, 1:250), Ly6C-BV605 (Biolegend #128035, 1:25), Ly6G-Pacific blue (Biolegend #127611, 1:100), CD11b-BUV737 (BD sciences #612800, 1:200), L/D blue (Invitrogen #L23105, 1:50), CD45.2-PECy7 (Biolegend #109830, 5:100), G-CSF receptor-PE (Abcam #AB233582, 1:5) and PE isotype (BD sciences #550617, 1:100). Lymphocyte samples: B220-PerCPCy5.5 (Biolegend #103235, 5:100), CD8-FITC (Biolegend #100705, 1:500), CD3-BV786 (BD sciences #564010, 3:100), CD69-BV605 (Biolegend #104529, 5:100), CD4-APC (Biolegend 100411, 1:200), CD122-BUV737 (BD sciences #741730, 1:00), L/D blue (Invitrogen #L23105, 1:50), CD45.2-PECy7 (Biolegend 109830, 5:100), NK1.1-PE (Biolegend #156504, 1:20) and BV605 isotype (BD sciences #562778, 1:100). Lymphocyte activation samples: CD62L-PECy7 (BD Pharmingen #560516, 1:50), CD8-FITC (Biolegend #100705, 1:500), CD3-BV786 (BD sciences #564010, 3:100), Ghost-BV510 (Tonbobio #13-0870-T100), CD44-Pacific blue (Biolegend #103019, 1:100), CD45.2-APCCy7 (Sigma #MABF436, 5:100), B220-AlexaFluoro700, CD4-APC (Biolegend 100411, 1:200). Thymus samples: Ghost-BV510 (Tonbobio #13-0870-T100), CD45.2-APCCy7 (Sigma #MABF436, 5:100), Thy1.2-BV605 (Biolegend #140317, 1:100), CD4-PECy7 (Biolegend #100527, 1:200), CD8-FITC (Biolegend #100705, 1:500), CD44-Pacific blue (Biolegend #103019, 1:100), CD25 AlexaFluoro700 (Biolegend #102024, 1:100)

### Neutrophil Isolation for Electron Microscopy

VPS45 KI mice and their WT littermates were sacrificed at 9 weeks. Spleen and bone marrow cells were isolated as stated in Materials and Methods, flow cytometry, and

mouse tissue processing. After red blood cell lysis, cells were resuspended in 1 mL of PBS with 2% FBS and 1 mM EDTA. Then EasySep™ Mouse Neutrophil Enrichment Kit (Stem Cell Technologies #18000) instructions were followed (as seen [https://cdn.stemcell.com/media/files/pis/10000003730-PIS\\_01.pdf](https://cdn.stemcell.com/media/files/pis/10000003730-PIS_01.pdf)). In short, cells were resuspended to  $1 \times 10^8$  cells/ml in 0.5- 2 mL. Rat serum was added to the samples, 50  $\mu$ l/ml, and the samples were moved to a round-bottom tube. Enrichment cocktail was added, 50  $\mu$ l/ml, samples were mixed and incubated for 15 minutes at 4°C. Tubes were topped off to 2.5mls and cells were pelleted (300xg, 10mins, 4°C). Cells were resuspended to  $1 \times 10^8$  cells/ml with PBS with 2% FBS and 1 mM EDTA. Selection cocktail was added, 50  $\mu$ l/ml, samples were mixed and incubated at 4°C for 15mins. Magnetic beads were vortexed for 30 seconds and then added to the samples, 150  $\mu$ l/ml. Samples were incubated for 10 minutes at 4°C. Samples were then topped off to 2.5 mL and incubated with a magnet at room temperature. The sample with the magnet was then inverted, and the sample was collected in 15 ml tubes. The samples were then prepped for electron microscopy. Samples were pelleted (400xg, 5 mins, 4 °C) and resuspended in a 1:1 mixture of PBS with 2% FBS and 1 mM EDTA and EM fixative (2.5% glutaraldehyde). Cells were pelleted and resuspended in 1 mL EM fixative and brought to the EM Core Facility for further processing. EM images were captured, and differences between WT and KI were examined through a blinded study of the samples. Significance was determined using a Student's t-test.

### **CD8 T cell isolation for Transmission Electron Microscopy.**

KI mice and WT littermates were sacrificed at 9 weeks. Spleens were isolated and processed as stated previously in the methods and materials. After red blood cell lysis, cells were resuspended in 1 mL of PBS with 2% FBS and 1 mM EDTA. Then followed EasySep™ Mouse CD8+ T Cell Isolation Kit (STEMCELL Technologies #19853), instructions are as follows [10000003748-PIS\\_02.pdf \(stemcell.com\)](https://cdn.stemcell.com/media/files/pis/10000003748-PIS_02.pdf). In short, cells were resuspended to a concentration of  $1 \times 10^8$  cells/ml in a volume of .25-2ml. Rat serum was added to samples, 50  $\mu$ l/ml. Samples were transferred to a round-bottom tube. Isolation Cocktail was added to samples, 50  $\mu$ l/ml, and cells were incubated at room temperature for 10 minutes. RapidSpheres were vortexed, then added to samples at 125  $\mu$ l/ml and incubated at room temperature for 5 mins. The samples were then topped off to 2.5 mL. And incubated on the magnet for 2.5 minutes at room temperature. The magnet and sample were then inverted to collect samples in 15 mL tubes. The samples were then prepped for electron microscopy. Samples were pelleted (400xg, 5mins, 4 °C) and resuspended in a 1:1 mixture of PBS with 2% FBS and 1 mM EDTA and EM fixative. Cells were pelleted and resuspended in 1 mL EM fixative and brought to the EM Core Facility for further processing. EM images were captured, and differences between WT and KI were determined through a blinded study of the samples. Significance was determined using a Student's t-test.

### **Bone Marrow Chimeras.**

KI mice, WT littermates, and WT CD45.1 controls were sacrificed the day before chimeras were created via CO<sub>2</sub> and cervical dislocation according to protocols. The weight of the mice was recorded. The femur and tibia were removed from the mice, and

as much fat and muscle as could be removed was. The bones were stored in media overnight at 4°C. The next day, cells were collected from the bones, keeping everything sterile, working under the hood. Samples were resuspended in sterile PBS to a concentration of  $1 \times 10^7$  cells/200ml. Chimeric mice hosts were irradiated with 850 rads and allowed to rest for 4 hours. After this bone marrow graft solution was then injected via the tail vein of the mouse, 200ul into each host. Mice were then placed on antibiotic water and checked daily. Engraftment was completed by 2 months, and mice were then sacrificed. Chimeric mice were sacrificed and processed using complete blood counts on isolated blood immediately after collection.

## Bibliography

1. Gimeno-Agud, H., Diaz-Osorio, Y., Oyarzabal, A. Biological Basis of Cell Trafficking: A General Overview. *J In Met Dis.* **48**, e12839 (2025).
2. Costaguta G, Payne G. Overview of Protein Trafficking Mechanisms. *Trafficking Inside Cells: Pathways, Mechanisms and Regulation.* 105–14 (2009)
3. Kloepper, Tobias H, C. Nickias, Fasshauer, D. An Elaborate Classification of SNARE Proteins Sheds Light on the Conservation of Eukaryotic Endomembrane System. *Mol. Biol. Cell* **18**, 3463-3471 (2007).
4. Fasshauer, D., Sutton R. B., Brunger A. T., & Jahn R. Conserved Structural Features of Synaptic Fusion Complex: SNARE Proteins Reclassified as Q- and R-SNARES. *Proc. Natl. Acad. Sci.* **95**, 15781-15786 (1998).
5. Bock, J. B., Matern, H. T., Peden, A. A. & Scheller, R. H. A Genomic Perspective on Membrane Compartment Organization. *Nature.* **409**, 839-841 (2001).
6. Hong W. SNARES and Traffic. *Biochem. Biophys. Acta-Mol Cell Res.* **1744**, 120-144 (2005).
7. Furukawa, N. & Mima J. Multiple and Distinct Strategies of Yeast SNAREs to Confer the Specificity of Membrane Fusion. *Sci. Rep.* **4**, 1-13 (2014).
8. Xu, Y., Su, L. & Rizot, J. Binding of Munc 18-1 to Synaptobrevin and to the SNARE Four-helix Bundle. *Biochemistry* **49**, 1568-1576 (2010).
9. Misura, K. M., Scheller, R. H. & Weis, W. I. Three-dimensional Structure of the Neuronal-Sec1-syntaxin 1a Complex. *Nature* **404**, 355-362 (2000).
10. Aran V. *et al.* Characterization of Two Distinct Binding Modes Between Syntaxin 4 and Munc18c. *Biochem. J.* **419**, 655-660 (2009).
11. Munson, M. & Hughson, F. M. Conformational Regulation of SNARE Assembly and Disassembly in vivo. *J. Biol. Chem.* **277**, 9375-9381 (2002).
12. Paumet, F., Rahimian, V., Di Liberto, M. & Rothman, J. E. Concerted Auto-regulation in Yeast Endosomal t-SNAREs. *J. Biol. Chem.* **280**, 21237-21143 (2005).
13. Bryant, N. J. & James, D. E. Vps45p Stabilizes the Syntain Homologue Tlg2p and Positively Regulates SNARE Complex Formation. *EMBO J.* **20**, 3380-3388 (2001).
14. Struthers, M. L. *et al.* Functional Homology of Mammalian Syntaxin 16 and Yeast Tlg2 Reveals a Conserved Regulatory Mechanism. *J Cell Sci.* **122**, 2292-2299 (2009).
15. Fernandez I. *et al.* Three-dimensional Structure of an Evolutionarily Conserved N-terminal Domain of Syntaxin 1A. *Cell.* **94**, 841-849 (1998).

16. Munson, M., Chen, X., Cocina, A. E., Schultz, S. M. & Hughson, F. M. Interactions within the Yeast t-SNARE Sso1p that Controls SNARE Complex Assembly. *Nat. Struct. Biol.* **7**, 894-902 (2000).
17. Burkhardt, P., Hattendorf, D. A., Weis, W. I. & Fasshauer, D. Munc18a Controls SNARE Assembly Through its Interactions with Syntaxin N-peptide. *EMBO J.* **27**, 923-933 (2008).
18. MacDonald, C., Munson, M. & Bryant, N. J. Autoinhibition of SNARE Complex Assembly by a Conformational Switch Represents a Conserved Feature of Syntaxins. *Biochem. Soc. Trans.* **38**, 209-212 (2010).
19. Carpp, L. N., Ciufo, L. F., Shanks, S. G., Boyd, A. & Bryant, N. J. The Sec1/Munc18 Protein Vps45p Binds Its Cognate SNARE Protein via Two Distinct Modes. *J. Cell Biol.* **173**, 927-936 (2006).
20. Lobingier, B. T. & Merz, A. J. Sec1/Munc18 Protein Vps33 Binds to SNARE Complex. *Mol. Biol. Cell* **23**, 4611-4622 (2012).
21. Gossing, M., Chidambaram, S. & Fischer von Mollard, G. Importance of the N-Terminal Domain of the Qb-SNARE Vti1p for Different Membrane Transport Steps in the Yeast Endosomal System. *PLoS One* **8**. (2013).
22. Munson, M. & Bryant, N. J. A Role for the Syntaxin N-terminus: Figure 1. *Biochem. J.* **418**, e1-e3 (2009).
23. Wener, T. *et al.* SNAREpins: Minimal Fusion Machinery for Membrane Fusion. *Cell* **92**, 759-772 (1998).
24. Wendler, F. & Tooze, S. Syntaxin 6: The Promiscuous Behavior of a SNARE Protein. *Traffic* **2**, 606-611 (2001).
25. Togneri, J., Cheng, Y. S., Munson, M., Hughson, F. M., & Carr, C. M. Specific SNARE Complex Binding Mode of the Sce1/Munc18 Protein SEC1p. *Proc. Natl. Acad. Sci.* **103**, 17730-17735 (2006).
26. Baker, R. W. *et al.* A Direct role of the Sec1/Munc18-Family Protein Vps33 as a Template for SNARE Assembly. *Science*. **349**, 1111-1114 (2015).
27. Dulubova I, *et al.* Convergence and Divergence in the Mechanism of SNARE Binding by Sec1/Munc18-like Proteins. *Proc. Natl. Acad. Sci.* **100**, 32-37 (2003).
28. Carr, C. M. & Rizo, J. At the Junction of SNARE and SM Protein Function. *Curr. Opin. Cell Biol.* **22**, 519-527 (2010).
29. Hashizume, Krinstina, Cheng, Yi-Shan, Hutton, Jenna L., Chiu, Chi-hua, Carr, C. M. Yeast Sec1 Functions Before and After Vesicle Docking. *Mol. Biol. Cell.* **20**, 4673-4685 (2009).
30. Graham, S. C. *et al.* Structural Basis of Vps33A Recruitment to the Human HOPS Complex by Vps16. *PNAS.* **110(330)**. 13345-13350 (2013).
31. Peng, R. & Gallwitz, D. Sly1 Protein Bound to Golgi Syntaxin Sed5p Allows Assembly and Contributes to Specificity of SNARE Fusion Complexes. *J. Cell Biol.* **157(4)**. 645-655 (2002).

32. Eisemann, T. J., Allen, F., Lau, K., Shimamura, G. R., Jeffrey, P. D., Hughson, F. M. The Sec1/Munc18 Protein Vps45 Holds the Qa-SNARE Tlg2 in a Open Conformation. *elife*. **9**:e60724 (2020).
33. Hata, Yutaka, Slaughter, Clive A., Sudhof, T. C., Synaptic Vesicle Fusion Complex Contains unc-18 Holomogue Bound to Syntaxin. *Lett. to Nat.* **366**, 347-351 (1993).
34. Verhage M. Synaptic Assembly of the Brain in the Absence of Neurotransmitter Secretion. *Science* (80-.). **287**, 864-869 (2000).
35. Dulubova, I *et al.* A Conformational Switch in Syntaxin During Exocytosis: Role of Munc18. *EMBO J.* **18**, 4372-4382 (1999).
36. Richmond, J. E., Weimer, R. M. & Jorgensen, E. M. An Open Form of Syntaxin Bypasses the Requirement for UNC13 in Vesicle Priming. *Nature* **412**, 338-341 (2001).
37. Dulubova I. *et all.* How Tlg2p/Syntaxin 16 Snares Vps45. **21**, (2002).
38. Bracher, A. & Weissenhorn, W. Crystal Structure of Neuronal Squid Sec1 Implicate Inner-Domain Hinge Movement in the Release of t-SNAREs. *J. Mol. Biol.* **306**, 7-13 (2001).
39. Bracher, A, & Weissenhorn, W. Structural Basis for the Golgi Membrane Recruitment of Sly1p by Sed5p. *EMBO J.* **21**, 6114-6124 (2002).
40. Sadler J. B. A., Roccisana, J., Virolainen, M., Bryant, N. J., & Gould, G. W. mVps45 Knockdown Selectively Modulates VAMP Expression in 3T3-L1 Adipocytes. *Commun. Integr. Biol.* **8**, 2-5 (2015).
41. Frey *et al.* Mammalian VPS45 Orchestrates Trafficking Through the Endosomal System. *Blood.* **137**, 1932-1944 (2021).
42. Stepemsky P. *et al.* The Thr224Asn Mutation in VPS45 Gene is Associated with the Congenital Neutropenia and Primary Myelofibrosis of Infancy. *Blood.* **121**, 5078-5087 (2013).
43. Vilboux, T. *et al.* A Congenital Neutrophil Defect Syndrome Associated with Mutations in VPS45. *N.Engl. J Med.* **369**, 54-65 (2013).
44. Meerschaut, I. *et al.* Severe Congenital Neutropenia with Neurological Impairment Due to a Homozygous VPS45 p.E238K Mutation: A Case Report Suggesting a Genotype-Phenotype Correlation. *Am. J. Med. Genet. Part A* **167**, 3214-3218 (2015).
45. Shah, R. K. *et al.* A Novel Homozygous VPS45 p.P468L Mutation Leading to Severe Congenital Neutropenia with Myelofibrosis. *Pediatr. Blood Cancer* **64**, e26571 (2017).
46. Ueki, M *et al.* Severe Congenital Neutropenia-Type 5: Impaired T cell Proliferation, Aberrant Th1 Cytokine Production, Abnormal Megakaryocytes, and Impaired Platelet Granule Formation in a Patient with VPS45 Deficiency Caused by Uniparental Isodisomy. *Blood.* **142** 5382 (2023).

47. Skokowa, J. Dale, D. C., Touw, I. P., Zeidler, C. & Welte, K. Severe Congenital Neutropenias. *Nat. Rev. Dis. Prim.* **3**, 17032 (2017).
48. Stow, J. L., Manderson, A. P., Murray, R. Z. SNAREing Immunity: the Role of SNAREs in the Immune System. *Nature Reviews Immunology.* **6** 919-929 (2006)
49. Ashby, K. M. & Hogquist, K. A. A Guide to Thymic Selection of T cells. *Nature Reviews Immunology.* **24** 103-117 (2024).
50. Roccisana, J., Sadler, J. B. A., Bryant, N. J., Gould, G. W. Sorting of GLUT4 into its Insulin-Sensitive Stores Required the Sec1/Munc18 Protein mVps45. *Mol. Biol. Cell* **15** 2389-97 (2013).
51. Rahajeng, J., Caplan, S., Naslavsky, N. Common & Distinct Roles for the Binding Partners Rabenosyn-5 and Vps45 in the Regulation of Endocytic Trafficking in Mammalian Cells. *Exp Cell Res.* **316** 859-874 (2009).
52. D'Orlando, O. *et al.* Syntaxin 11 is required for NK and CD8+ T-cell Cytotoxicity and Neutrophil Degranulation. *Eur J. Immunol.* **43** 194-208 (2012).
53. Spessott, W. A., Sanmillan, M. L., Kulkarni, U. U., McCormick, M. E., Giraudo, C. G. Syntain 4 Mediates Endosome Recycling for the Lytic Granules Exocytosis in Cytotoxic T-lymphocytes. *Traffic* **18** 442-452 (2017).